JOURNAL OF GEOPHYSICAL RESEARCH, VOL. 115, D00M02, doi:10.1029/2009JD013728, 2010

Review of the formulation of present-generation stratospheric chemistry-climate models and associated external forcings

O. Morgenstern,[1] M. A. Giorgetta,[2] K. Shibata,[3] V. Eyring,[4] D. W. Waugh,[5] T. G. Shepherd,[6] H. Akiyoshi,[7] J. Austin,[8,9] A. J. G. Baumgaertner,[10] S. Bekki,[11] P. Braesicke,[12] C. Brühl,[10] M. P. Chipperfield,[13] D. Cugnet,[11] M. Dameris,[4] S. Dhomse,[13] S. M. Frith,[14] H. Garny,[4] A. Gettelman,[9] S. C. Hardiman,[15] M. I. Hegglin,[6] P. Jöckel,[4] D. E. Kinnison,[9] J.-F. Lamarque,[9] E. Mancini,[16] E. Manzini,[17] M. Marchand,[11] M. Michou,[18] T. Nakamura,[7] J. E. Nielsen,[14] D. Olivié,[18] G. Pitari,[16] D. A. Plummer,[19] E. Rozanov,[20,21] J. F. Scinocca,[19] D. Smale,[1] H. Teyssèdre,[18] M. Toohey,[22] W. Tian,[13] and Y. Yamashita[7]

Received 18 December 2009; revised 15 March 2010; accepted 29 March 2010; published 14 August 2010.

[1] The goal of the Chemistry-Climate Model Validation (CCMVal) activity is to improve understanding of chemistry-climate models (CCMs) through process-oriented evaluation and to provide reliable projections of stratospheric ozone and its impact on climate. An appreciation of the details of model formulations is essential for understanding how models respond to the changing external forcings of greenhouse gases and ozone-depleting substances, and hence for understanding the ozone and climate forecasts produced by the models participating in this activity. Here we introduce and review the models used for the second round (CCMVal-2) of this intercomparison, regarding the implementation of chemical, transport, radiative, and dynamical processes in these models. In particular, we review the advantages and problems associated with approaches used to model processes of relevance to stratospheric dynamics and chemistry. Furthermore, we state the definitions of the reference simulations performed, and describe the forcing data used in these simulations. We identify some developments in chemistry-climate modeling that make models more physically based or more comprehensive, including the introduction of an interactive ocean, online photolysis, troposphere-stratosphere chemistry, and non-orographic gravity-wave deposition as linked to tropospheric convection. The relatively new developments indicate that stratospheric CCM modeling is becoming more consistent with our physically based understanding of the atmosphere.

Citation: Morgenstern, O., et al. (2010), Review of the formulation of present-generation stratospheric chemistry-climate models and associated external forcings, *J. Geophys. Res.*, *115*, D00M02, doi:10.1029/2009JD013728.

[1]National Institute of Water and Atmospheric Research, Lauder, New Zealand.
[2]Max-Planck-Institut für Meteorologie, Hamburg, Germany.
[3]Meteorological Research Institute, Japan Meteorological Agency, Tsukuba, Japan.
[4]Deutsches Zentrum für Luft- und Raumfahrt, Institut für Physik der Atmosphäre, Wessling, Germany.
[5]Department of Earth and Planetary Sciences, John Hopkins University, Baltimore, Maryland, USA.
[6]Department of Physics, University of Toronto, Toronto, Ontario, Canada.
[7]National Institute of Environmental Studies, Tsukuba, Japan.
[8]National Oceanic and Atmospheric Administration, Princeton, New Jersey, USA.
[9]National Center for Atmospheric Research, Boulder, Colorado, USA.
[10]Max-Planck-Institut für Chemie, Mainz, Germany.
[11]LATMOS, IPSL, UVSQ, UPMC, CNRS, INSU, Paris, France.
[12]NCAS-Climate-Chemistry, Centre for Atmospheric Science, Department of Chemistry, Cambridge University, Cambridge, UK.
[13]School of Earth and Environment, University of Leeds, Leeds, UK.
[14]NASA Goddard Space Flight Center, Greenbelt, Maryland, USA.
[15]Hadley Centre, Met Office, Exeter, UK.
[16]Dipartimento di Fisica, Università degli Studi dell'Aquila, L'Aquila, Italy.
[17]Centro Euro-Mediterraneo per i Cambiamenti Climatici, Bologna, Italy.
[18]GAME, CNRM, Météo-France, CNRS, Toulouse, France.
[19]Canadian Centre for Climate Modeling and Analysis, Environment Canada, Victoria, British Columbia, Canada.
[20]Physical-Meteorological Observatory/World Radiation Center, Davos, Switzerland.
[21]Institut für Atmosphäre und Klima, ETH Zurich, Zurich, Switzerland.
[22]Leibniz-Institut für Meereswissenschaften an der Universität Kiel (IFM-GEOMAR), Kiel, Germany.

0148-0227/10/2009JD013728

1. Introduction

[2] To predict the future evolution of stratospheric ozone and attribute its behavior to the different forcings, models are required that can adequately represent both the chemistry of the ozone layer and the dynamics and energetics of the atmosphere, as well as their natural variability. The coupling of stratospheric chemical models with climate models has led to a new generation of models far more complex than those available when the Montreal Protocol was signed in 1987. Such models, known as coupled Chemistry-Climate Models (CCMs) are used within the Chemistry-Climate Model Validation activity 2 (CCMVal-2) [*Eyring et al.*, 2008] and represent both stratospheric chemistry and atmospheric climate. Coupling both processes in a single model allows the study of feedback processes between these two components, for example addressing the question of how global climate change, associated with the production of anthropogenic greenhouse gases (GHGs), will interfere with ozone recovery as anticipated under the terms of the Montreal Protocol and its amendments. However, coupling these two processes into a single model complicates the interpretation of results, compared to models that treat the processes separately (chemistry-transport models and general circulation models (GCMs)). In particular, the models' responses to external forcings depend on details of the model setup as well as the applied forcings.

[3] The goal of CCMVal is to improve understanding of CCMs and their underlying GCMs through process-oriented evaluation, along with discussion and coordinated analysis of science results (http://www.pa.op.dlr.de/CCMVal). CCMVal-2 represents the second phase of the CCMVal activity. The CCMVal-1 activity was conducted in 2005/2006 in support of *World Meteorological Organization* (*WMO*) [2007] and resulted in a comprehensive assessment of the state-of-the-art of modeling the ozone layer and associated phenomena using 11 different climate models [e.g., *Eyring et al.*, 2006, 2007; *WMO*, 2007; *Austin et al.*, 2008; *Son et al.*, 2008; *Struthers et al.*, 2009]. CCMVal-1 produced the most authoritative forecast of the evolution of the ozone layer to date. However, also some major model deficiencies were exposed, for example associated with the transport schemes used by the models, resulting in non-conservation of chemical tracers. Also anthropogenic ozone depletion likely started before 1980, the start date for the reference simulations of CCMVal-1. Limited computing resources meant that most simulations ended in 2050 or earlier, excluding the period when ozone will probably be substantially affected by ozone super-recovery associated with global climate change [*Shepherd*, 2008]. Finally, only a limited set of diagnostic results was produced which for example would prevent analysis of the occurrence of short-lived extreme events, such as sudden stratospheric warmings. To address these deficiencies, CCMVal-2 is designed to more fully capture the period of anthropogenic ozone depletion and its interaction with climate change, comprising the period of 1960–2100, and a more comprehensive list of diagnostic output has been produced, including daily mean and instantaneous fields. In addition, in the years since CCMVal-1 model development has been targeted at the deficiencies identified there.

[4] For the CCMVal-2 model simulations, external forcings have been defined, a recommendation about chemical kinetic data has been provided, and a wider range of diagnostics has been requested. External forcings include surface abundances of ozone-depleting substances (ODS) and GHGs, emissions of ozone and aerosol precursors, stratospheric aerosol, variations in solar output, and ocean surface conditions. The Quasi-Biennial Oscillation (QBO) of tropical stratospheric winds is also prescribed in some CCMs not spontaneously producing a QBO, or to adjust its phase. Some of these forcings should be considered internal to the climate system (particularly the ocean surface conditions and the QBO). Imposing these affects any interpretation of climate signals discerned from the CCMVal-2 simulations. The set of forcings needed for the CCMVal-2 simulations partly reflects the state-of-the-art of chemistry-climate modeling, the subject of this paper. For example, if in the future models routinely simulate the QBO or include an interactive ocean, the corresponding forcings will no longer be needed.

[5] In the present paper, we provide high-level documentation on the models participating in the CCMVal-2 modeling activity, relying on information collected in support of CCMVal-2. There are too many different approaches taken in CCM modeling, and too many processes to consider for it to be feasible to document the technical details of every model within the limitations of a single paper. Therefore, here we focus on general approaches taken, and also on unusual aspects of individual models. Some of these unusual aspects can be considered progressive (meaning closer to our physical understanding of the climate system than other, conventional approaches) and illustrating how CCMs may evolve in the future. We will address specific advantages of, or problems associated with particular methods only in general terms; assessing the results produced by the models is the subject of other papers such as the ones in this special section, [e.g., *Austin et al.*, 2010; *Gettelman et al.*, 2010; *Gerber et al.*, 2010; *Hegglin et al.*, 2010; *Morgenstern et al.*, 2010a].

[6] The paper is structured as follows: In section 2 we briefly review the major components that make up a CCM (dynamics, radiation, chemistry, transport). Section 3 contains introductions of all CCMVal-2 models, focussing on the unusual aspects of these models. Section 4 outlines the simulations performed for CCMVal-2 and the external data used for the simulations. We present some concluding remarks in section 5.

2. Major Components of Chemistry-Climate Models

[7] The major building blocks of CCMs are the dynamical core, physical processes (e.g., radiation, convection, boundary layer processes, and cloud physics), the transport scheme, and the chemistry and microphysics modules associated with chemical composition change. These major components are linked by feedback processes, e.g. radiatively active chemical tracers feeding into radiation, or circulation changes affecting chemical composition [*WMO*, 2007, Figure 5-1]. For explanations of model names and associated institutions see Table 1. Table 2 lists the basis GCMs of the CCMVal-2 models. Several models share a common heritage. The E39CA, EMAC, and SOCOL models are all based on the ECHAM GCM. (Note that SOCOL simulations have been contributed by two different groups; their model setups

Table 1. CCMVal-2 Models (Acronym, Full Name) and Associated Centers of Model Development

CCM	Full Name	Institution
AMTRAC3	Atmospheric Model with TRansport and Chemistry 3	NOAA, Princeton, USA
CAM3.5	Community Atmosphere Model 3.5	NCAR, Boulder, USA
CCSRNIES	Center for Climate System Research/National Institute for Environmental Studies	NIES, Tsukuba, Japan
CMAM	Canadian Middle Atmosphere Model	Environment Canada, Victoria, and U. Toronto, Canada
CNRM-ACM	Centre National de Recherches Météorologiques - ARPEGE-Climat coupled MOCAGE	Météo-France, Toulouse, France
E39CA	ECHAM4.L39(DLR)/CHEM/-ATTILA	DLR, Oberpfaffenhofen, Germany
EMAC	ECHAM/MESSy Atmospheric Chemistry model	MPI-Chemistry, Mainz, and DLR, Oberpfaffenhofen, Germany
GEOSCCM	Goddard Earth Observing System - Chemistry-Climate Model	NASA GSFC, Greenbelt, USA
LMDZrepro	Laboratoire de Météorologie Dynamique Zoom – REPROBUS	IPSL, Paris, France
MRI	Meteorological Research Institute	JMA, Tsukuba, Japan
Niwa-SOCOL	National Institute of Water and Atmospheric Research - Solar-Climate-Ozone Links	NIWA, Lauder, New Zealand
SOCOL	Solar-Climate-Ozone Links	PMOD/WRC, Davos, and ETH Zürich, Switzerland
ULAQ	Universitá degli Studi dell'Aquila	U. L'Aquila, Italy
UMSLIMCAT	Unified Model – SLIMCAT	U. Leeds, UK
UMETRAC	Unified Model with Eulerian Transport and Atmospheric Chemistry	NIWA, Lauder, NZ
UMUKCA-METO	Unified Model/U. K. Chemistry Aerosol Community Model - Met Office	Met Office, Exeter, UK
UMUKCA-UCAM	Unified Model/U. K. Chemistry Aerosol Community Model - U. Cambridge	U. Cambridge, UK, and NIWA, Lauder, NZ
WACCM	Whole-Atmosphere Chemistry-Climate Model	NCAR, Boulder, USA

differ in some respects, as detailed below. Where this distinction is not necessary, the two models SOCOL and Niwa-SOCOL are collectively referred to as "(Niwa-)SOCOL".) UMETRAC, UMSLIMCAT, and UMUKCA models are based on the Unified Model (UM). (UMUKCA simulations have been contributed by two different groups; the simulations are referred to as UMUKCA-METO and UMUKCA-UCAM. Collectively, we refer to the model as "UMUKCA".) However, both ECHAM and the UM have undergone substantial development in recent years, such that models based on the newer versions of these models (EMAC, UMUKCA) may behave quite differently from those based on the older versions (E39CA, (Niwa-)SOCOL, UMETRAC, UMSLIMCAT). CAM3.5 and WACCM are both based on the NCAR CAM/CLM. The other models may be regarded as independent; however, models typically share approaches to certain problems with other models (see below).

2.1. Dynamics

2.1.1. Dynamical Cores and Coordinate Systems

[8] Dynamical cores describe the temporal evolution of wind, temperature and pressure, or equivalent variables, under the influences of inertia in a rotating framework, gravity, and different diabatic and topographic forcings. The development of dynamical cores was initially strongly pushed by the needs in numerical weather prediction (NWP), with an emphasis on accurate and highly efficient numerical methods for solving, in most cases, the hydrostatic primitive equations. In NWP models, the spectral transform method [e.g., *Holton*, 1992] is widely used, because for a relatively

Table 2. CCMVal-2 Models, With Reference, Horizontal Resolution, Number of Levels, and Name of Parent GCM

CCM	Reference	Hor. Res., Levels	Top of Model	Base Model
AMTRAC3	*Austin and Wilson* [2006]	~200 km, L48	0.017 hPa	AM3
CAM3.5	*Lamarque et al.* [2008]	1.9° × 2.50°, L26	3.5 hPa	CAM
CCSRNIES	*Akiyoshi et al.* [2009]	T42L34	0.012 hPa	CCSR/NIES AGCM 5.4 g
CMAM	*Scinocca et al.* [2008]	T31L71	0.00081 hPa	AGCM3
CNRM-ACM	*Teyssèdre et al.* [2007], *Déqué* [2007]	T42L60	0.07 hPa	ARPEGE-Climat 4.6
E39CA	*Stenke et al.* [2008, 2009]	T30L39	10 hPa	ECHAM4
EMAC	*Jöckel et al.* [2006]	T42L90	0.01 hPa	ECHAM5
GEOSCCM	*Pawson et al.* [2008]	2.0° × 2.50°, L72	0.015 hPa	GEOS5
LMDZrepro	*Jourdain et al.* [2008]	2.5° × 3.75°, L50	0.07 hPa	LMDz
MRI	*Shibata and Deushi* [2008a, 2008b]	T42L68	0.01 hPa	MJ98
(Niwa-)SOCOL	*Schraner et al.* [2008]	T30L39	0.01 hPa	MAECHAM4
ULAQ	*Pitari et al.* [2002]	R6L26	0.04 hPa	ULAQ-GCM
UMETRAC	*Austin and Butchart* [2003]	2.5° × 3.75°, L64	0.01 hPa	UM 4.5
UMSLIMCAT	*Tian and Chipperfield* [2005]	2.5° × 3.75°, L64	0.01 hPa	UM 4.5
UMUKCA	*Morgenstern et al.* [2009]	2.5° × 3.75°, L60	84 km	UM 6.1
WACCM	*Garcia et al.* [2007]	1.9° × 2.50°, L66	6×10^{-6} hPa	CAM

small number of degrees of freedom it allows accurate and numerically very efficient simulations of baroclinic waves that are a major concern for weather forecasting. Hence, this method is also frequently used in atmospheric GCMs for climate research, because of its advantageous performance at low resolution, and is used by roughly half of the CCMVal-2 models (CCSRNIES, CMAM, CNRM-ACM, E39CA, EMAC, MRI, (Niwa-)SOCOL, ULAQ). The transport equation is however not easily treated in a spectral coordinate system, due to the occurrence of numerical artifacts [*Rasch and Williamson*, 1990]; hence some models using the spectral transform method perform transport in physical space (E39CA, EMAC, MRI, (Niwa-)SOCOL). Likewise, parameterized and explicit physical processes are difficult to implement in spectral models.

[9] Almost all of the remaining models use a regular latitude-longitude grid, favored because it allows for a straightforward discretization of the governing equations. Disadvantages are a non-uniform resolution and special treatments required at the poles [e.g., *Lanser et al.*, 2000]. The AMTRAC3 uses a "cubed sphere" grid [*Putman and Lin*, 2007; *Adcroft et al.*, 2007], based on projecting the edges of a cube onto a sphere around its center.

[10] The dynamical cores of most CCMs are based on the hydrostatic primitive equations [e.g., *Holton*, 1992], with terrain-following hybrid-pressure as the vertical coordinate. The Met Office's New Dynamics Unified Model (UMUKCA) solves a non-hydrostatic set of equations [*Davies et al.*, 2005], although UMUKCA is used at a resolution that would justify the hydrostatic approximation. This also results in UMUKCA being the only model using hybrid-height as the vertical coordinate system (i.e., near the surface, the model levels follow the orography, but in the stratosphere are pure height levels). The ULAQ CCM uses a quasi-geostrophic set of equations [*Pitari*, 1993], which introduces errors in the large-scale dynamics, especially in the tropics. Also ULAQ uses non-terrain following pressure.

2.1.2. Horizontal Diffusion

[11] Diffusion is generally split into horizontal and vertical diffusion. Horizontal diffusion is often necessary as closure for the discretized horizontal dynamics, which accumulates energy at the resolution limit. Depending on the details of the dynamical core, this is achieved implicitly (GEOSCCM, UMUKCA [*McCalpin*, 1988]) or by an explicit horizontal diffusion term (all other CCMVal-2 models). Due to the lack of a general theory of turbulence, horizontal diffusion schemes are quite different in their characteristics, but they achieve the main purpose of suppressing dynamic instabilities with the least possible impact on large scale features of the general circulation. Models with spectral transform dynamics often apply high-order diffusion operators (of order ∇^4 or higher) to be scale selective (CNRM-ACM, E39CA, EMAC, (Niwa-)SOCOL), while those grid point models that need explicit diffusion rely on low order operators (e.g., ∇^2), which can be realized with small stencils (i.e., using few grid points for the application of the diffusion operator; CAM3.5, LMDZrepro, WACCM).

[12] "Sponges", i.e. increased diffusivity near the model top, are often necessary to reduce the artificial reflection of atmospheric waves off the model top and are used in the majority of CCMVal-2 models. Depending on the formulation of the sponge, their effects may however extend to lower layers and violate angular momentum conservation [*Shepherd et al.*, 1996; *Shepherd and Shaw*, 2004]. Such effects can be avoided if the sponge does not affect the zonal mean structures (EMAC, CMAM). Some models do not need an additional sponge at the model top (GEOSCCM, MRI, UMUKCA). Further aspects of numerical diffusion are discussed below in the context of advection schemes.

2.1.3. Quasi-biennial Oscillation

[13] The QBO is the major dynamical mode of variability of the tropical stratosphere and gives rise to QBO signals in circulation and chemistry in many other regions of the atmosphere [*Baldwin et al.*, 2001; *Giorgetta and Bengtsson*, 1999]. The QBO results from wave mean-flow interaction, which reinforces the westerly and easterly jets of the QBO and causes their downward propagation against the general upwelling in the tropical stratosphere. In recent years, a number of climate models have simulated the QBO [*Takahashi*, 1999; *Scaife et al.*, 2000; *Giorgetta et al.*, 2002; *McLandress*, 2002]. These approaches require a relatively high vertical resolution in the stratosphere and an adequate parameterization of gravity wave drag (section 2.1.4). For the class of CCMs used for CCMVal-2, the QBO remains a challenge [*Giorgetta et al.*, 2006]. The major difficulty in simulating the QBO arises from the imperfect representation of tropical convection, which in reality excites a broad spectrum of vertically propagating waves. While CCMs can resolve the large-scale portion of this spectrum if a suitable vertical resolution is used, a realistic excitation of these waves also depends strongly on the spatial and temporal characteristics of the simulated convection, and therefore on the parameterization of convection [*Horinouchi et al.*, 2003]. The contribution of unresolved waves to the wave mean-flow interaction in the QBO shear layers depends entirely on parameterizations of gravity waves. While the simulation of the wave mean-flow interaction is considered to be the biggest challenge, also the tropical upwelling needs to be simulated well, to allow for a realistic quasi-biennial period of the equatorial oscillation in the zonal wind [*Giorgetta et al.*, 2006].

[14] In the CCMVal-2 simulations, the QBO is only imposed in some models in the simulations about reproducing the past (section 4.2.2). In these simulations, the CCMVal-2 models fall into two categories: One group of models does not impose an observed QBO, either because the QBO is internally generated, as in cases of MRI and the the UM-based models (UMETRAC, UMSLIMCAT, and UMUKCA [*Scaife et al.*, 2000]), or because some models do not have any representation of the QBO (AMTRAC3, CMAM, CNRM-ACM, LMDZrepro). A second group of models uses nudging to a climatology (section 4.3.5) to externally impose the QBO in these simulations (CAM3.5, CCSRNIES, E39CA, EMAC, (Niwa-)SOCOL, ULAQ, WACCM). EMAC is a special case here in that it spontaneously produces a QBO [*Giorgetta et al.*, 2006] but nudging is merely used to adjust the phase. Note that at 58 days the timescale of nudging in EMAC is much longer than those chosen for the other models, which are typically between 5 and 10 days; also nudging is restricted to a smaller vertical domain than in the other models. At 5 to 10 days the nudging timescales of the other models are similar to those of large-scale equatorial waves, whose unrealistic representation (due to insufficient vertical resolution and/or

Table 3. Non-orographic Gravity Wave Drag in CCMVal-2 Models

CCM	GWD Reference
AMTRAC3	*Alexander and Dunkerton* [1999]
CAM3.5	*Richter et al.* [2010]
CCSRNIES	*Hines* [1997a]
CMAM	*Scinocca* [2003]
CNRM-ACM	*Bossuet et al.* [1998]
E39CA	NA[a]
EMAC	*Hines* [1997a, 1997b]
GEOSCCM	*Garcia and Boville* [1994]
LMDZrepro	*Lott et al.* [2005]
MRI	*Hines* [1997a]
(Niwa-)SOCOL	*Charron and Manzini* [2002]
ULAQ	Rayleigh friction
UMETRAC	*Scaife et al.* [2000]
UMSLIMCAT	*Scaife et al.* [2000]
UMUKCA	*Scaife et al.* [2002]
WACCM	*Richter et al.* [2010]

[a]NA, not applicable.

excitation by tropical weather) is an important reason for the absence of a QBO in some models.

[15] QBO nudging has however limitations: (1) By construction, the nudging of zonal wind may introduce localized momentum sources and sinks, thus violating the internal momentum budget of the atmosphere. (2) The QBO is an internal mode of variability, but nudging makes the QBO dependent on boundary conditions. This will destroy any internal variability arising from two-way interaction with the extratropics [*Anstey et al.*, 2010]. (3) Nudging generally results in a realistic zonally averaged structure of the QBO, but does not repair the potentially deficient wave structures in the wind fields of the models. QBO nudging can therefore contribute to QBO signals related to zonal mean effects, but not to QBO signals dependent on waves, e.g., eddy fluxes of tracers. (4) Simulations covering the future cannot use nudging to observations.

2.1.4. Gravity Wave Drag

[16] Gravity wave drag (GWD) is among the drivers of meridional overturning in the middle atmosphere, also known as the Brewer-Dobson Circulation [*McIntyre*, 1995], and of the QBO (section 2.1.3). The small spatial scales and complications due to wave breaking in the mesosphere require their effects to be parameterized. Gravity waves are excited by tropospheric processes, mainly flow over topography and convection. Hence GWD parameterizations are usually divided into two parts, orographic and non-orographic. CAM3.5, CNRM-ACM, and WACCM link GWD to tropospheric convection [*Bossuet et al.*, 1998; *Richter et al.*, 2010]; in the other models, this link is not incorporated. *McLandress and Scinocca* [2005] examine the impacts on middle-atmosphere dynamics of three different GWD schemes [*Hines*, 1997a; *Alexander and Dunkerton*, 1999; *Warner and McIntyre*, 2001], variants of which are widely used across the CCMVal-2 models (Table 3). The three schemes, when employed in a comparable way, produce very similar dynamical responses despite differences in the dissipation mechanisms. This suggests that differences in responses to GWD are mainly due to adjustable parameters in the schemes, such as the properties of the launch spectrum or the launch height, but not the dissipation mechanism. E39CA does not have a representation of non-orographic GWD because of the low top in this model. ULAQ represents the effect of GWD through Rayleigh friction, which violates momentum conservation [*Shepherd and Shaw*, 2004]. Momentum conservation can also be violated in flux-based GWD parameterizations if momentum flux is allowed to escape out the top of the model domain [*Shaw and Shepherd*, 2007].

2.2. Radiation

[17] Radiative processes lead to additional challenges in the development of CCMs. Traditionally separate radiative transfer schemes are used for shortwave heating and photolysis; this is the case in all CCMVal-2 models except CAM3.5, CCSRNIES, and WACCM. Radiative transfer schemes for shortwave heating often use relatively broad spectral bands covering the solar spectrum from the near infrared to the UV, and include scattering by air molecules and cloud and aerosol particles [e.g., *Edwards and Slingo*, 1996]. Radiative transfer schemes used for photolysis (section 2.3.5) need to resolve the UV spectrum much better, and scattering may be treated differently [e.g., *Lary and Pyle*, 1991]. All models use the two-stream approximation for short-wave radiation (a common simplification used in radiative transfer modeling). An inspection of the number of spectral bands, both in the shortwave and the longwave part of the spectrum, reveals substantial differences in spectral resolution. Models that cover the upper atmosphere (WACCM, CMAM) also include chemical heating (i.e. the heating produced by some exothermic/endothermic chemical reactions, which is typically ignored at lower levels [*Marsh et al.*, 2007]) and non-local thermodynamical equilibrium (non-LTE) effects, produced e.g. by excitation of vibrational states of molecules under conditions of low collision probability (low density) [*Kockarts*, 1980; *Fomichev et al.*, 1998].

2.3. Chemistry and Composition

2.3.1. Chemical Schemes

[18] All models participating in CCMVal-2 employ an inorganic chemistry scheme including chlorine chemistry; all but the E39CA model also contain an explicit representation of bromine chemistry. In the E39CA model bromine chemistry is parameterized [*Steil et al.*, 1998; *Stenke et al.*, 2009]. The number and type of source gases for chlorine and bromine varies greatly between models. Lumping (i.e., adding the halogen atoms of those source gases not represented in the chemistry schemes to those that are, with similar lifetimes) is used widely across the CCMVal-2 models; only AMTRAC3, CCSRNIES, CNRM-ACM, (Niwa-)SOCOL, and UMETRAC do not use it. Particularly for UMSLIMCAT and UMUKCA lumping has a big impact on the few halogen sources gases (CFC-11, CFC-12, CH_3Br) represented in their schemes [*Chipperfield*, 1999] since for present-day conditions, these three gases only account for roughly half of total stratospheric chlorine and bromine, respectively. AMTRAC3 and UMETRAC do not represent the halogen source species directly, but the local rate of change of inorganic chlorine and bromine are calculated using tabulated functions of the derivatives of the source molecules with respect to the stratospheric age of air [*Austin and Butchart*, 2003; *Austin et al.*, 2010]. Although modelers have been asked to update their kinetics data to *Sander et al.* [2006],

few have done so completely and most use a mixture of different sources. Other sources of kinetic data used in CCMVal-2 models include *DeMore et al.* [1997], *Sander et al.* [2002], International Union of Pure and Applied Chemistry (Evaluated Kinetic Data, International Union of Pure and Applied Chemistry Subcommittee for Gas Kinetic Data Evaluation, various years; available at http://www.iupac-kinetic.ch.cam.ac.uk) and a variety of other sources. Reasons for not upgrading a model to the recommended data include that the upgrade can be difficult or time-consuming, or would make the model incompatible with earlier versions.

2.3.2. Tropospheric Composition

[19] The major target of CCMVal-participating models is the stratosphere; hence tropospheric chemistry is simplified or absent in most models. This is motivated by the success e.g. of stratospheric chemistry-transport models in broadly reproducing stratospheric ozone without considering tropospheric chemistry [e.g., *Chipperfield*, 1999]. However, the absence of tropospheric chemistry in most CCMVal-2 models must be regarded as a limitation. Only CAM3.5, EMAC, and ULAQ include a comprehensive representation of tropospheric chemistry; these models are however characterized by low resolution (ULAQ), a low model top (CAM3.5), or few simulations (EMAC). This reflects the added cost imposed by tropospheric chemistry. In the other models, tropospheric composition is handled in a variety of ways: Introduction of background tropospheric chemistry/methane oxidation (AMTRAC3, CCSRNIES, MRI, (Niwa-)SOCOL, UMUKCA, WACCM); relaxation of tropospheric ozone and/or other constituents to a climatology (AMTRAC3, GEOSCCM, CNRM-ACM, LMDZrepro, UMETRAC); or the treatment of chemical species as passive tracers below a specified level (CMAM, UMSLIMCAT).

2.3.3. Upper-Atmospheric Composition

[20] Processes specific to the upper atmosphere include ion chemistry, solar particle precipitation associated with NO_x production, and other effects. Mesospheric NO_x production is thought to affect NO_y abundances in the stratospheric polar vortex [*Vogel et al.*, 2008] although its magnitude is uncertain and dependent on solar activity. Only WACCM has explicit representations of these upper-atmospheric processes [*Garcia et al.*, 2007]. EMAC, MRI, and WACCM treat the production of NO_x by cosmic rays and solar particles in the mesosphere; CMAM takes this into account by imposing an upper boundary condition for NO_x of 1 ppmv.

2.3.4. Time-Integration of Chemical Kinetics

[21] Homogeneous reactions (i.e. reactions between free-moving gas phase molecules) are represented by simultaneous first-order, first-degree, homogeneous ordinary differential equations. Unlike atmospheric dynamics, atmospheric chemical kinetics is generally predictable with well-defined steady state solutions which, in the absence of transport, transient states usually converge to [*Shepherd*, 2003]. Chemical reactions are however stiff in that the lifetimes of individual species vary by many orders of magnitude [e.g., *Jacobson*, 1999]. To obtain stable and accurate solutions for such stiff chemical equations, different numerical methods have been used in atmospheric chemistry. Most popular is the family method [e.g., *Austin*, 1991; *Ramaroson et al.*, 1992], adopted by all CCMVal-2 models except CAM3.5, CMAM, EMAC, (Niwa-)SOCOL, UMUKCA, and WACCM. This method relies on the fact that there are groups (families) of gases, namely the odd oxygen (O_x), odd hydrogen (HO_x), odd nitrogen (NO_x, NO_y), chlorine (ClO_x), and bromine (BrO_x) families, within which family members are linked by fast reactions (meaning that equilibrium assumptions can be made), but the lifetimes of the families as a whole are much longer. As a result, families are treated as long-lived species and can be integrated with a long time step. Indeed, the family method is accurate for moderate- and low-stiffness systems, but, to be so, the families need to be carefully set up and validated. The grouping of species into families for chemistry does not need to correspond to any grouping adopted for transport [*de Grandpré et al.*, 1997; *Dameris et al.*, 2005].

[22] By contrast, the non-family methods, used by CAM3.5, CMAM, EMAC, (Niwa-)SOCOL, UMUKCA, and WACCM, make no such a priori assumption about lifetimes. Advantages of non-family chemistry include the possibility to extend the chemistry scheme into the upper atmosphere (where the family assumption is not valid). Solvers in this category comprise a Rosenbrock-type predictor-corrector method (EMAC), a combined explicit-implicit Backward-Euler method (CAM3.5, CMAM, WACCM), and the Newton-Raphson iterative method ((Niwa-)SOCOL, UMUKCA).

2.3.5. Photolysis

[23] There are two commonly used methods for the calculation of photolysis rates, the online and the off-line (look-up table) methods. Off-line methods involve filling, for every photolysis reaction included in the model, a table of photolysis rates as functions of pressure, solar zenith angle (SZA), overhead ozone column, and often temperature [e.g., *Lary and Pyle*, 1991]. SZAs up to 100° are taken into consideration because angles larger than 90° are important for polar spring ozone depletion triggered by solar radiation which reaches the stratosphere earlier than the Earth's surface, due to the Earth's curvature. The tables are filled off-line or once at the start of a simulation. Interpolation then yields the photolysis rates at any time and location of the model simulation. This method is computationally efficient; however, it usually limits the number and types of physical effects that can be considered. For example, surface albedo, clouds, and aerosols are often assumed uniform [e.g., *Chipperfield*, 1999]. If solar cycle effects are included, the photolysis tables need to be updated periodically, or the phase of the 11-year cycle needs to be among the interpolation parameters (AMTRAC3).

[24] By contrast, models using online photolysis schemes (CAM3.5, CCSRNIES, EMAC, E39CA, WACCM) evaluate the radiative transfer equation at the time of simulation, accounting for variations in cloudiness, albedo, and solar output [e.g., *Landgraf and Crutzen*, 1998; *Bian and Prather*, 2002]. As noted before, CAM3.5, CCSRNIES, and WACCM treat photolysis and shortwave radiation consistently, whereas the other models calculate shortwave radiation and photolysis separately, possibly leading to inconsistencies e.g. in the placement of the terminator or the absorption cross sections underlying both formulations.

2.3.6. Heterogeneous Reactions and PSC Microphysics

[25] Certain chemical reactions proceed efficiently between gas molecules and adsorbed or substrate molecules in the surface layer of liquid or solid aerosol particles. Such reactions are called heterogeneous. The heterogeneous reactions are described by a first-order loss process for the gas reactant,

Table 4. PSC Microphysics in CCMVal-2 Models[a]

CCM	Particles	NAT/Ice Sedimentation Velocity (mm/s)	Thermodynamics
AMTRAC3	NAT/ice/SAD	0.14/12.7	EQ
CAM3.5	NAT/ice/STS	radius-dependent	NAT: HY; ice: EQ
CCSRNIES	NAT/ice/STS	radius-dependent	EQ
CMAM	ice/STS	NA/0	ice: EQ
CNRM-ACM	NAT/ice/LSA	ice: ~17.3	EQ
E39CA	NAT/ice/LSA	*Steil et al.* [1998]	HY
EMAC	NAT/ice/LSA	*Buchholz* [2005]	NAT: HY; ice: EQ
GEOSCCM	NAT/ice/LSA	radius-dependent	HY
LMDZrepro	NAT/ice/LA	*Lefèvre et al.* [1998]	EQ
MRI	NAT/ice/SO_4	0.17/17.4	EQ
(Niwa-)SOCOL	NAT/ice/LSA	*Schraner et al.* [2008]	EQ
ULAQ	NAT/ice/SAD	radius-dependent	HY
UMSLIMCAT	NAT/ice/STS	0.46/17.3	EQ
UMETRAC	NAT/ice/SAD	0.14/12.7	EQ
UMUKCA	NAT/ice/SO_4	0.46/17.3	EQ
WACCM	NAT/ice/STS	radius-dependent	EQ

[a]Types of particles considered, sedimentation velocities of PSCs, and assumptions for thermodynamics. EQ = thermodynamic equilibrium. HY = Hysteresis/non-equilibrium effects considered. NAT = nitric acid trihydrate. SAD = sulphuric acid dihydrate. STS = supercooled ternary solution. LSA = liquid supercooled aerosol. LA = liquid aerosol. The different abbreviations reflect different assumptions made about stratospheric sulfate aerosol, the surface area density of which is prescribed. Where a sedimentation velocity is not explicitly stated, no fixed sedimentation velocity is imposed, as described in the references listed, or the sedimentation velocity is particle-size dependent. NA, not applicable.

and the rate constant is proportional to the thermal velocity of the gas molecules, the particulate surface area density (SAD), and an uptake coefficient. The uptake coefficient is dimensionless with a value between 0 and 1, and typically depends on temperature and pressure [*Sander et al.*, 2006].

[26] In the CCMVal-2 models, two types of particles, sulfate aerosols and polar stratospheric clouds (PSCs), are considered in the stratosphere. Sulfate aerosols result from oxidation of sulfur-containing precursors (e.g., carbonyl sulfide) during volcanically clean periods; in addition, explosive volcanic eruptions can cause temporary increases in the sulfate aerosol abundance by orders of magnitude [e.g., *Robock*, 2002]. The absence of representations of stratospheric aerosol physics and chemistry in CCMVal-2 models means that sulfate aerosol needs to be externally imposed. PSCs, on the other hand, are internal variables, and there are large differences among CCMs for their treatments, regarding their formation mechanisms, types, and sizes (Table 4). All CCMs include water-ice PSCs; all except CMAM also include $HNO_3 \cdot 3\ H_2O$ (nitric acid trihydrate, NAT). Most CCMs furthermore treat sulfate aerosols, e.g. in the form of supercooled ternary solutions (STS) of sulfuric acid (H_2SO_4), nitric acid (HNO_3), and water. Heterogeneous reactions also differ between CCMs. The most important reactions for chlorine activation ($ClONO_2 + H_2O$; $ClONO_2$ + HCl; HOCl + HCl) and N_2O_5 hydrolysis leading to HNO_3 formation are present in all models. The treatment of reactions involving bromine is less consistent; this may be because heterogeneous activation of bromine is less important than that of chlorine due to the non-existence of a photochemically stable inorganic reservoir for bromine (as is HCl for chlorine [*Brasseur et al.*, 1999]).

[27] The conditions at which PSCs condense and evaporate vary, not only for water-ice PSCs but also for NAT and STS, between CCMs (Table 4). The simplest assumption is that PSCs are formed at the saturation points of HNO_3 over NAT and H_2O over water-ice. This assumption is made in most CCMVal-2 CCMs. By contrast, the ULAQ model does not assume thermodynamic equilibrium and thus allows for supersaturation and other non-equilibrium effects. ULAQ has 9 tracers each for size-resolved NAT and ice [*Pitari et al.*, 2002]. CAM3.5 and WACCM also allow for supersaturation of up to 10 times saturation but do not transport a separate NAT tracer [*Garcia et al.*, 2007]. GEOSCCM accounts for non-equilibrium by using a NAT tracer. In EMAC, NAT only forms on ice or pre-existing NAT [*Buchholz*, 2005]. The equilibrium assumption only defines the mass of condensed PSC; assumptions about size distributions and particle shapes need to be made to derive surface area densities. The assumed size distribution affects the PSC sedimentation velocities, i.e., the rates of de-/rehydration and de-/renitrification, particularly in the case of large particles. The denitrification through PSC sedimentation contributes to the enhancement of polar stratospheric ozone loss in spring by inhibiting the formation of the $ClONO_2$ reservoir. All CCMs except CMAM include this process (Table 4) although sedimentation velocities differ a lot between models.

2.3.7. Surface Boundary Conditions, Emissions and Surface Sinks

[28] Different methods are used to impose source gases at the Earth' surface. For reproducing the past, GHGs and ODSs (CO_2, N_2O, CH_4, CFCs, halons) are prescribed at the surface using observed global-mean surface abundances. The same holds true for the future except that here the abundances are based on future projections. This method assures the source gas abundances near the surface to be close to the desired values. Diagnosed fluxes associated with the prescribed surface abundances may however substantially deviate from those derived from emission inventories; this would indicate a mismatch in lifetime for such a species between the CCM and the assessment model used to calculate the scenario. Models with an explicit or simplified treatment of tropospheric chemistry usually impose explicit emissions (fluxes) for higher organic species (represented in CAM3.5, EMAC, and ULAQ), NO_x, CO, and/or CH_2O. Emissions aloft by lightning [*Price and Rind*, 1992, 1994; *Müller and Brasseur*, 1995; *Grewe et al.*, 2001] or aircraft are also represented to a varying degree in those models. Emissions of SO_2, dimethyl sulfide (DMS) and NH_3 are

Table 5. Transport Scheme, by Tracer[a]

CCM	Physical Tracers	Water Vapor	Other Chemical Tracers	References
AMTRAC3	FFSL	FFSL	FFSL	*Lin* [2004]
CAM3.5	FFSL	FFSL	FFSL	*Lin* [2004]; *Rasch et al.* [2006]
CCSRNIES	STFD	STFD	STFD	*Numaguti et al.* [1997]
CMAM	Spectral	Spectral - log(q)	Spectral	
CNRM-ACM	SL, cubic	SL cubic	SL cubic	*Déqué* [2007]; *Williamson and Rasch* [1989]
E39CA	SL	ATTILA	ATTILA	*Reithmeier and Sausen* [2002]
EMAC	FFSL	FFSL	FFSL	*Lin and Rood* [1996]
GEOSCCM	FFSL	FFSL	FFSL	*Lin and Rood* [1996]
LMDZrepro	FV	FV	FV	*Hourdin and Armengaud* [1999]
MRI	STFD	STFD	Hybrid SL quintic and PRM	*Shibata and Deushi* [2008b]
(Niwa-)SOCOL	SL	SL	Hybrid	*Zubov et al.* [1999]; *Williamson and Rasch* [1989]
ULAQ	FFEE	FFEE	FFEE	
UMETRAC		Quintic FV	Quintic FV	*Gregory and West* [2002]
UMSLIMCAT		Quintic FV	Quintic FV	*Gregory and West* [2002]
UMUKCA	SL, quasi-cubic	SL. Hor.: quasi-cubic Vert.: quintic	As water vapor	*Priestley* [1993]
WACCM	FFSL	FFSL	FFSL	*Lin* [2004]

[a]FV = finite volume. FFSL = flux-form semi-Lagrangian. SL = semi-Lagrangian. STFD = spectral transform and finite difference. FFEE = flux form Eulerian explicit.

associated with tropospheric aerosol represented in CAM3.5, EMAC, ULAQ, UMETRAC, and UMUKCA.

[29] There are two types of deposition in the troposphere, dry deposition and wet deposition. Dry deposition may be represented by a deposition velocity for a particular surface and gas so that a deposition flux is the product of deposition velocity and abundance [e.g., *Walcek et al.*, 1986]. Dry deposition is an important component of the tropospheric ozone budget [e.g., *Hough*, 1991]. Wet deposition, on the other hand, involves the scavenging of gases by cloud droplets. Hydrohalogens such as HCl and HBr dissolve well in water; this makes wet deposition of these species the dominant sink for the reactive halogen species Cl_y and Br_y. Similarly, the wet deposition of HNO_3 is a major sink of total reactive nitrogen (NO_y).

[30] The removal of inorganic halogen is handled in different ways in the models. Most models (except AMTRAC3, CMAM, CNRM-ACM, GEOSCCM, LMDZrepro, UMETRAC and UMSLIMCAT) incorporate explicit washout (at least for some species) and dry deposition. CMAM is the only model to represent dry but not wet deposition. In some models removal is represented by relaxing species to a background tropospheric climatology (CNRM-ACM, LMDZrepro, UMETRAC). In the case of UMUKCA-UCAM, removal of inorganic halogens is achieved by imposing zero surface boundary conditions for these species [*Morgenstern et al.*, 2009]. In the UMUKCA-METO model, washout of inorganic halogen compounds is handled incorrectly, leading to a high bias of total chlorine and bromine in this model.

2.4. Advective Transport

[31] Advection is one of the major processes determining the distribution of chemical species, particularly in the lower stratosphere. Here the chemical lifetimes of long-lived species are much longer than the dynamical (transport) lifetimes, as manifested, for example, by the tape-recorder signal of H_2O in the equatorial lower stratosphere [*Mote et al.*, 1996] and by the "mixing barriers" in the subtropics and around the winter pole [e.g., *Shepherd*, 2007]. Hence differences in advection schemes may cause large differences in the distribution of chemical species and age of air [*Eluszkiewicz et al.*, 2000; *Gregory and West*, 2002; *Struthers et al.*, 2009]. In addition, inconsistencies may arise from the different discretization of the continuity equation and the tracer transport equation, as shown for example by *Jöckel et al.* [2001].

[32] Table 5 provides an overview of advection schemes used by the CCMVal-2 models. Several types of advection schemes are used in the CCMVal-2 models, namely finite volume, spectral, semi-Lagrangian, flux-form semi-Lagrangian, and fully Lagrangian schemes. Some CCMs (CNRM-ACM, E39CA, LMDZrepro, MRI, and (Niwa-)SOCOL) use different advection schemes for meteorological (i.e. momentum, heat, water) and chemical tracers, resulting in different numerical diffusivities for tracers advected by different schemes, and possible inconsistencies.

[33] Spectral advection in the horizontal and finite difference advection in the vertical (CCSRNIES, CMAM) conserves species mass but requires careful attention to avoid the development of sharp gradients in species distribution and to fill negative values [*de Grandpré et al.*, 2000].

[34] Semi-Lagrangian schemes can be used with relatively long time steps without compromising stability. Also semi-Lagrangian schemes are advantageous when a large number of tracers needs to be advected (such as in CCMs) because a major fraction of the cost is independent of the number of tracers. However, these schemes may be overly diffusive [e.g., *Eluszkiewicz et al.*, 2000] due to an interpolation step necessary to project tracers from the departure points onto the arrival points. This diffusive property can be improved through higher-order interpolation, e.g. quintic (MRI, UMUKCA [*Priestley*, 1993]). However, the better accuracy of higher-order interpolation comes at the price of numerical artifacts, such as overshoots and undershoots (similar to those found in spectral advection), which require special treatment. Also, semi-Lagrangian schemes tend to exhibit non-conservation of tracers, requiring a correction. By contrast, flux-form semi-Lagrangian advection is considered relatively accurate and is conserving tracers; however, in practice little difference has been found between flux-form semi-Lagrangian and spectral advection schemes [*Eyring et al.*, 2006; *Shepherd*, 2007]. Flux-form schemes

are used in a number of models (AMTRAC3, CAM3.5, EMAC, GEOSCCM, WACCM). If set up appropriately, they conserve tracers. Many models in this category (AMTRAC3, CAM3.5, EMAC, GEOSCCM, WACCM) use formulations after *Lin and Rood* [1996, 1997] or *Lin* [2004]. LMDZrepro, UMETRAC, and UMSLIMCAT use finite-volume advection schemes [*Hourdin and Armengaud*, 1999; *Gregory and West*, 2002].

[35] The E39CA model uses a fully Lagrangian approach to constituent transport, thereby avoiding the interpolation step needed in semi-Lagrangian methods [*Reithmeier and Sausen*, 2002; *Stenke et al.*, 2008, 2009]. This method is not subject to numerical diffusion, thus allowing for a specification of explicit, physically motivated diffusion to represent mixing between neighboring parcels. This explicitly defined diffusion may be much smaller than numerical diffusion found in other schemes. The ATTILA scheme in E39CA is characterized by decreasing parcel density (i.e., effectively decreasing resolution) with height. This main disadvantage needs to be weighed against the gain of representing diffusion as a physical process characterizing the atmosphere, not a numerical artifact.

3. Models Used in CCMVal-2

[36] The following lists the major features of CCMVal-2 models, particularly those that can be considered unusual or progressive, compared to the other models. The participating CCMs are listed in Table 2 and are described in detail in the cited literature.

[37] 1. The AMTRAC3 model is based on a cubed-sphere grid [*Putman and Lin*, 2007], so it is the only model using neither a latitude-longitude grid nor a spectral representation. AMTRAC3 does not explicitly represent halocarbon species; instead, the release of chlorine and bromine (updated from *Austin and Wilson* [2006] and *Austin et al.* [2010]) is parameterized as a function of age-of-air.

[38] 2. CAM3.5 is based on the CAM climate model, with a low model top at 3.5 hPa. CAM3.5 comprises a comprehensive stratospheric and tropospheric chemistry package based on a non-families formulation of chemistry [*Kinnison et al.*, 2007; *Lamarque et al.*, 2008]. Photolysis is calculated online, consistent with short-wave radiation [*Kinnison et al.*, 2007]. Gravity-wave drag depends on tropospheric convection [*Richter et al.*, 2010]. CAM3.5 uses a mass-conserving flux-form formulation of advection [*Lin*, 2004]. Hysteresis is considered in NAT formation [*Kinnison et al.*, 2007].

[39] 3. The CCSRNIES model originates from a numerical weather prediction model developed at the Japan Meteorological Agency. Some improvements of the codes and an extension of heights up to the stratosphere were made for the GCM in CCSR. CCSRNIES uses online photolysis, treating shortwave radiation and photolysis consistently [*Akiyoshi et al.*, 2009]. CCSRNIES has the most comprehensive representation of heterogeneous reactions involving bromine [*Akiyoshi et al.*, 2009].

[40] 4. CMAM is the only CCMVal-2 model coupled to an interactive ocean [*Gent et al.*, 1998; *Arora et al.*, 2009]. NAT PSC formation and the associated denitrification are not included in CMAM [*Hitchcock et al.*, 2009]. CMAM accounts for mesospheric NO_x production by cosmic rays/solar particles by imposing an upper boundary condition at ~94 km for NO_x of 1 ppmv. CMAM uses a non-families formulation of chemistry [after *de Grandpré et al.*, 2000].

[41] 5. The CNRM-ACM uses two different grids for dynamics and chemistry (T42 versus T21), to reduce computational cost. Dynamical coupling between dynamics and chemistry is performed via a 6-hourly exchange of fields [*Déqué*, 2007; *Teyssèdre et al.*, 2007]. GWD in the CNRM-ACM includes a component dependent on tropospheric convection [*Bossuet et al.*, 1998].

[42] 6. E39CA is the only CCMVal-2 model employing a fully Lagrangian advection scheme [*Reithmeier and Sausen*, 2002; *Stenke et al.*, 2009] which is strictly mass conserving and non-diffusive. The top lid in E39CA is at 10 hPa; E39CA does not have any non-orographic GWD implemented in the model. Bromine chemistry in E39CA is parameterized [*Stenke et al.*, 2009]. E39CA uses an online photolysis scheme [*Landgraf and Crutzen*, 1998]. Hysteresis is considered in NAT formation [*Steil et al.*, 1998].

[43] 7. The EMAC model operates at a very high vertical resolution (48 levels between 100 and 1 hPa). EMAC includes a comprehensive representation of tropospheric chemistry [*Jöckel et al.*, 2006] as well as mesospheric production of NO_x. Chemistry is formulated in a non-families framework in EMAC, using a Rosenbrock solver. EMAC uses online photolysis [*Landgraf and Crutzen*, 1998]. Hysteresis is considered in NAT formation [*Buchholz*, 2005].

[44] 8. GEOSCCM is based on the GEOS5 GCM. It does not use explicit diffusion and also does not have a sponge layer. PSC microphysics in GEOSCCM accounts for supersaturation. Tropospheric chemistry is imposed, using a climatology [*Logan*, 1999]. Photolysis is calculated online [*Douglass et al.*, 1997].

[45] 9. LMDZrepro couples the atmospheric component of the IPSL Earth System model [*Lott et al.*, 2005] to the REPROBUS chemical mechanism [*Lefèvre et al.*, 1998]. PSC microphysics assumes a bimodal size distribution of the PSC particles [*Lefèvre et al.*, 1998]. Different advection schemes are used for meteorological and chemical tracers. Tropospheric composition is imposed below 400 hPa, following *Savage et al.* [2004].

[46] 10. The MRI model uses reduced explicit diffusivity in the stratosphere [*Shibata and Deushi*, 2008a]. Transport in this spectral model is performed using a semi-Lagrangian advection scheme satisfying the continuity equation [*Xiao and Peng*, 2004]. The MRI model does not use a sponge layer.

[47] 11. The (Niwa-)SOCOL CCM is a spectral model using semi-Lagrangian transport for the chemical constituents [*Zubov et al.*, 1999]. Chemistry is integrated using a non-families solver [*Egorova et al.*, 2003]. NAT particle number density is capped to account for supersaturation in NAT clouds. Photolysis is calculated online [*Rozanov et al.*, 1999]. Niwa-SOCOL differs from SOCOL in some details of photochemistry, and in the sea surface conditions applied (section 4.3.1).

[48] 12. ULAQ is a low-resolution CCM based on quasi-geostrophic dynamics, using a spectral representation with rhomboidal truncation [*Pitari et al.*, 2002]. ULAQ incorporates a comprehensive tropospheric and stratospheric chemistry, as well as a representation of NAT microphysics involving 9 NAT and 9 ice tracers. GWD is considered using Rayleigh friction. Photolysis is calculated online [*Pitari et al.*, 2002].

[49] 13. UMETRAC is based on a vertically expanded version of the climate model HadCM3, with added interactive stratospheric chemistry [*Austin and Butchart*, 2003]. Organic halogen species are not included; instead, the production of inorganic halogen is parameterized based on an age-of-air tracer [*Austin and Wilson*, 2006].

[50] 14. UMSLIMCAT consists of the middle-atmosphere version of HadCM3 coupled to the chemistry part of the SLIMCAT CTM [*Tian and Chipperfield*, 2005]. Stratospheric water vapor is coupled to the GCM's humidity field.

[51] 15. UMUKCA is based on the New Dynamics Unified Model, i.e. it uses non-hydrostatic dynamics and hybrid-height as the vertical coordinate [*Davies et al.*, 2005]. There is no explicit diffusion and no sponge layer in UMUKCA [*McCalpin*, 1988]. Chemistry is based on the UKCA package [*Morgenstern et al.*, 2009], a comprehensive stratospheric mechanism implemented using a non-families solver. Due to a warm temperature bias at the tropical tropopause, water vapor is prescribed in this region [*Morgenstern et al.*, 2009]. UMUKCA-METO has tropospheric washout of inorganic halogen implemented albeit incorrectly. UMUKCA-UCAM uses older photochemical data than UMUKCA-METO.

[52] 16. WACCM, v.3.5.48, extends into the lower thermosphere, employing a comprehensive middle- and upper-atmosphere chemistry mechanism [*Kinnison et al.*, 2007]. Transport uses a mass-conserving flux-form algorithm [*Lin*, 2004]. Heating due to volcanic aerosols is derived consistently from the aerosol surface area density. Photolysis is calculated online [*Kinnison et al.*, 2007], and photolysis and shortwave radiation are consistent with each other. GWD has a component dependent on tropospheric convection [*Richter et al.*, 2010].

4. Simulations Conducted for CCMVal-2

[53] In this section, we motivate and state the definitions of the model simulations defined for CCMVal-2 and discuss the associated forcings. The CCMVal community has defined reference and sensitivity simulations that are carried out in support of upcoming ozone and climate assessments and that are tailored to the SPARC CCMVal report on the evaluation of coupled Chemistry-Climate Models (CCMs) [*Eyring et al.*, 2008]. The overriding principle behind the choice of the reference simulations is to produce the best possible science. Accordingly, the first requirement is to evaluate the models against observations. That is the rationale behind "REF-B0", a time-slice experiment performed under year-2000 conditions, the period for which the largest wealth of observations is available. A long reference run will provide robust statistics for the model comparison. The second requirement is to see how well the models can reproduce the past behavior of stratospheric ozone. That is the rationale for the transient reference simulation "REF-B1", which is forced by observations. *Eyring et al.* [2006] show that it is important to establish a good baseline from which to identify the effects of halogens on ozone, and to avoid spin-up problems. Based on this experience, REF-B1 requires around 10-years spin-up prior to a 1960 start. The third requirement is to use the models to predict the future evolution of stratospheric ozone. That is the rationale for the transient reference simulation "REF-B2", which is forced by trace gas projections and modeled sea surface temperatures (SSTs). *Eyring et al.* [2007] suggest that it is important to have a continuous time series from the models covering both past and future, in order to avoid inhomogeneity in the data sets (in terms of both absolute values and variability), and also that the simulations extend to 2100 in order to fully capture the process of ozone recovery from the effects of ozone-depleting substances (ODSs). Based on this experience, REF-B2 also requires around 10-years spin-up prior to a 1960 start, and extension to 2100. To provide continuity with *Eyring et al.* [2007], and track any changes in the models, REF-B2 is based on the same GHG scenario (SRES A1B [*Intergovernmental Panel on Climate Change* (*IPCC*), 2001]) as used by *Eyring et al.* [2007]. The A1B scenario is based on the assumptions, for the 21st century, of rapid economic growth, further population increase until 2050 and a decline thereafter, global adoption of efficient technologies, and a balanced reliance on fossil- and non-fossil-fuel energy sources. In comparison to other SRES scenarios, this scenario results in a middle-of-the-road increase in anthropogenic radiative forcing.

4.1. Internal and External Modeling Uncertainties

[54] A source of error in CCMVal integrations relates to deficiencies in model formulation. Using identical boundary conditions, differences in the formulation of CCMs will lead to differences in their common prognostic or diagnostic fields. These differences will represent the internal uncertainties in dynamics, physics and chemistry in CCMs as used here. The CCMVal-2 simulations "REF-B0" and "REF-B1" (section 4.2), covering the near-present and the past, respectively, have been designed primarily to address internal modeling uncertainties since SSTs, sea ice, and other external forcings such as volcanic eruptions and variations of solar irradiance, are prescribed based on observations. By contrast, the "REF-B2" simulations, covering the past and future, also include external uncertainty because here SST and sea ice data are obtained from climate simulations, with associated biases (section 4.2.3). In REF-B0 and REF-B1, there are also external uncertainties associated with the construction of observational forcings (e.g., caused by instrument errors, lack of coverage, or other problems). Further external uncertainties in REF-B2 are associated with the future GHG and ODS forcings assumed. Furthermore, internal model uncertainties can also be associated with the methodology used in applying external forcings, which can be difficult to implement and vary among the models; this applies to all simulations.

4.2. CCMVal-2 Simulations

[55] The three reference simulations noted above and six control and sensitivity experiments have been proposed [*Eyring et al.*, 2008]. The reference simulations have been performed by most models, some with more than one ensemble member (CMAM, MRI, SOCOL, ULAQ, and WACCM, for the REF-B2 simulations). The sensitivity simulations are designed to explore particular scientific questions, such as, how would the ozone layer evolve taking into account short-lived source gases of stratospheric bromine (SCN-B1), under a different GHG scenario (SCN-B2a), under the influence of climate change but with invariant ODSs (SCN-B2b), with changing ODSs but with constant GHGs (SCN-B2c), and taking into account natural variability due to the QBO and the

Table 6. Ocean Surface Forcings Used for REF-B2 in CCMVal-2 Models

CCM	Ocean Forcing	Reference
AMTRAC3	CM2	*Delworth et al.* [2006]
CAM3.5	CCSM3	*Collins et al.* [2006]
CCSRNIES	MIROC/IPCC-AR4	*Shiogama et al.* [2005]; *Nozawa et al.* [2007]
CMAM	Interactive	*Arora et al.* [2009]
CNRM-ACM	CNRM-CM3 AR4 A1B	*Madec et al.* [1998]
E39CA	HadGEM1	*Stott et al.* [2006]
GEOSCCM	CCSM3	*Collins et al.* [2006]
LMDZrepro	IPSL-CM4 (see text)	*Dufresne et al.* [2005]
MRI	MRI-CGCM2.3.2	*Yukimoto et al.* [2006]
Niwa-SOCOL	HadISST1/HadGEM1	*Rayner et al.* [2003]; *Johns et al.* [2006]
SOCOL	ECHAM5-MPIOM	*Roeckner et al.* [2003, 2004]
ULAQ	CCSM3	*Collins et al.* [2006]
UMSLIMCAT	HadGEM1	*Johns et al.* [2006]
UMUKCA	HadGEM1	*Johns et al.* [2006]
WACCM	CCSM3	*Collins et al.* [2006]

solar cycle in the future (SCN-B2d). Furthermore, a 1960 time slice experiment (CNTL-B0) is suggested. For details about the sensitivity and control experiments, see *Eyring et al.* [2008].

4.2.1. REF-B0: Year 2000 Time-Slice Simulation

[56] REF-B0 is a time-slice simulation for 2000 conditions, designed to facilitate the comparison of model output against constituent data sets from various high-quality observational data sources and meteorological analyses under a period of high chlorine loading. Each simulation is integrated over 20 annual cycles following 10 years of spin-up. The surface concentrations of GHGs are based on SRES scenario A1B of *IPCC* [2001] while the surface halogens are based on Table 8-5 (scenario A1) of *WMO* [2007] for the year 2000. Both ODSs and GHGs repeat every year. Background aerosol is prescribed from the extended *Stratospheric Processes and Their Role in Climate* (*SPARC*) [2006] SAD data set (see section 4.3) for the year 2000. Solar irradiance is averaged over one solar cycle to provide a mean solar flux for the year 2000. Sea surface temperatures (SSTs) and sea ice concentrations (SICs) in this simulation are prescribed as a mean annual cycle derived from the years 1995 to 2004 of the HadISST1 data set [*Rayner et al.*, 2003]. Emissions of ozone and aerosol precursors (CO, NMVOC, NO_x and SO_2) are averaged over the years 1998 to 2000 and are taken from an extended data set of the REanalysis of the TROpospheric chemical composition (RETRO) project [*Schultz et al.*, 2007]. In case of SO_2, RETRO only provides biomass burning related emissions. Therefore, this data is combined with an interpolated version of EDGAR-HYDE 1.3 [*van Aardenne et al.*, 2001] and EDGAR 32FT2000 [*Olivier et al.*, 2005].

4.2.2. REF-B1: Reproducing the Past

[57] REF-B1 (1960–2006) is defined as a transient run from 1960 (with a 10-year spin-up period) to the present. All forcings in this simulation are taken from observations, and are similar or identical to those used by *Eyring et al.* [2006]. This transient simulation includes all anthropogenic and natural forcings based on changes in trace gases, solar variability, volcanic eruptions, and SSTs/SICs. GHGs (N_2O, CH_4, and CO_2) between 1950 and 1996 are taken from *IPCC* [2001] from 1997 to 2006 are NOAA observations (http://www.esrl.noaa.gov/gmd/aggi/). NOAA CO_2, CH_4, and N_2O are scaled to agree on January 1996 with the historical IPCC data. ODSs (CFC-10, CFC-11, CFC-12, CFC-113, CFC-114, CFC-115, CH_3CCl_3, HCFC-22, HCFC-141b, HCFC-142b, Halon-1211, Halon-1202, Halon-1301, and Halon-2402) are prescribed at the surface according to Table 8-5 of *WMO* [2007]. With the exceptions of AMTRAC3, CCSRNIES, CNRM-ACM, (Niwa-)SOCOL, and UMETRAC, the halogen contents of included source gases are adjusted for the halogen contents of source gases of similar lifetime which are not represented, such that model inputs for total chlorine and total bromine match the time series of total chlorine and bromine. This also applies to the other simulations. SSTs and SICs are prescribed as monthly mean boundary conditions following the observed global SIC and SST data set HadISST1 [*Rayner et al.*, 2003]. To correct for the loss of variance due to the time interpolation of monthly mean data, a variance correction is applied (http://grads.iges.org/c20c/c20c_forcing/karling_instruct.html), although many models did not include this. Aerosol SADs from observations are considered in REF-B1 (section 4.3.4). Stratospheric warming and tropospheric-surface cooling due to volcanic eruptions are either calculated online by using aerosol data or by prescribing heating rates and surface forcing. Solar variability is considered, using the data set described in section 4.3.6. CAM3.5, CCSRNIES, E39CA, EMAC, (Niwa-)SOCOL, ULAQ, and WACCM externally impose a QBO for REF-B1 (sections 2.1.3, 4.3.5). Ozone and aerosol precursors (CO, non-methane volatile organic carbons, NO_x and SO_2) from 1960 to 1999 are taken from the extended data set of the RETRO project [*Schultz et al.*, 2007]. After 2000 trend estimates taken from IIASA are used to extend the data set (P. Rafaj, personal communication, 2008). More details are in section 4.3.3.

4.2.3. REF-B2: Making Predictions

[58] REF-B2 is an internally consistent simulation covering 1960–2100, using only anthropogenic forcings. The objective of REF-B2 is to produce best estimates of the future ozone-climate change assuming scenario SRES A1B for GHGs and decreases in halogen emissions (adjusted Scenario A1). GHGs follow the *IPCC* [2001] SRES A1B scenario, as in the work by *Eyring et al.* [2007]. ODSs are based on scenario A1 from *WMO* [2007]. However, at the 2007 Meeting of the Parties to the Montreal Protocol, the Parties agreed to an earlier phase out of HCFCs (http://ozone.unep.org/Meeting_Documents/mop/19mop/Adjustments_on_HCFCs.pdf). Scenario A1 does not include this phase out. Hence, a new scenario has been developed that includes this phase out (hereafter referred to as the "adjusted scenario A1"). CFCs, Halons, and other non-HCFC species remain as in the original scenario A1 (section 4.3.2). Sulfate aerosol is the same as in REF-B0, i.e., background, non-volcanic aerosol loading is assumed. Regarding ocean forcing, due to potential discontinuities between the observed and modeled data record, the REF-B2 runs use simulated SSTs and SICs for the entire period, using GCM simulations forced with the SRES A1B GHG scenario (Table 6; section 4.3.1), or in the case of CMAM, an interactive ocean. The same variance correction as in REF-B1 has been requested. Ozone and aerosol precursors are identical to REF-B1 until 2000 and use the adjusted IIASA scenario through to 2100 (P. Rafaj, personal communication, 2008).

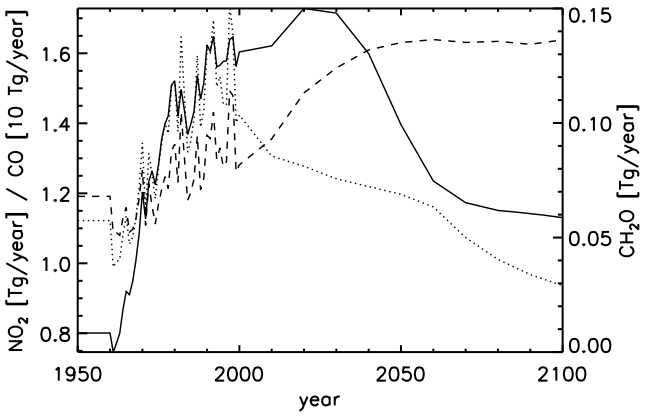

Figure 1. Surface emissions of NO_x (solid) (displayed as TG/year of NO_2), CO (dotted) and CH_2O (dashed) as used for CCMVal-2 simulations. From 1960 to 1999 these are from the RETRO emissions database (see text); after 1999 they are extrapolates using the IIASA scenario SRES A1B. Before 1960 they are just repeated 1960 RETRO emissions. Reproduced from *Morgenstern et al.* [2010b].

4.3. External Forcings

4.3.1. SSTs and Sea Ice

[59] REF-B0 and REF-B1 use the HadISST1 observational SST/sea ice data set (http://hadobs.metoffice.com/hadisst). It covers the period of 1870-present; a comprehensive description is given by *Rayner et al.* [2003]. Almost all simulations in these categories use HadISST1. There is a distinctive warming trend in the HadISST1 SSTs, starting at around 1970. Since then, the sea surface has warmed by 0.2 to 0.3 K, in the global mean. LMDZrepro uses AMIP II seas surface data [*Taylor et al.*, 2000] to force the REF-B0 and REF-B1 simulations. Three (of 4) MRI REF-B1 simulations use MRI CGCM 2.3.2 SSTs and sea ice data [*Yukimoto et al.*, 2006].

[60] For the REF-B2 simulations modelers use a variety of different data sets, or, in the case of CMAM, an interactive ocean model. Mean SSTs from the HadGEM1 climate model [*Johns et al.*, 2006] exhibit a cold bias of around 2 K versus HadISST1. This bias, and various other biases found in other climate model data, are the reason why a seamless simulation of past and future climate and ozone, such as REF-B2, cannot be performed based on a combination of analyzed and simulated SSTs. Two groups of models sharing the same ocean surface forcing in REF-B2 appear, namely CAM3.5, GEOSCCM, ULAQ, and WACCM all use CCSM3 data, while E39CA, UMSLIMCAT, and the UMUKCA models use HadGEM1 data (Table 6). Niwa-SOCOL uses a combination of HadISST1 and HadGEM1 SSTs for its ocean forcing of REF-B2, introducing a discontinuity into this simulation.

[61] For the LMDZrepro REF-B2 simulation, sea surface conditions are taken from the A1b simulation produced with the IPSL AOGCM [*Dufresne et al.*, 2005]. Since this simulation exhibits biases with respect to the AMIP II data set [*Taylor et al.*, 2000], the mean biases for the 1985–2005 period are first removed from the entire A1b simulation and then the corrected SST and sea ice forcing is used to force LMDZrepro.

4.3.2. Long-Lived Greenhouse Gases and Ozone-Depleting Substances

[62] The ODSs increase sharply during the 1970s and 1980s, resulting in an approximate six-folding of organic chlorine and a doubling of organic bromine at peak abundances in the 1990s, relative to preindustrial times. For the 21st century, according to the "adjusted A1" scenario, a continuous decline, in accordance with the Montreal Protocol, is anticipated. The decline is substantially slower than the increase in the 20th century. By contrast, in the A1B scenario [*IPCC*, 2001], for CO_2 a steady increase is anticipated, leading to a more than doubling by 2100, compared to 1950. N_2O follows a similar trend, albeit with smaller growth rates. CH_4, however, is anticipated to reduce after around 2050.

4.3.3. Ozone Precursors

[63] Surface emissions of NO_x, CO, and CH_2O, as used by many models, are displayed in Figure 1. For the period from 1960 to 1999 the data are from the RETRO database [*Schultz et al.*, 2007]. For the 21st century, the IIASA SRES A1B scenario forecasts a general decrease in CO emissions. NO_x emissions are forecast to peak around 2020, followed by a sharp decrease. Emissions of CH_2O are anticipated to increase then stabilize during the second half of the century. The interannual variability characterizing the RETRO emissions is absent in the 21st century. The decrease in NO_x and CO emissions, and the stabilization of emissions of CH_2O, reflect a declining trend in fossil-fuel usage throughout the 21st century. The IIASA emissions are courtesy of Peter Rafaj, IIASA (http://www.ozone-sec.ch.cam.ac.uk/ccmval_emissions).

[64] CAM3.5, E39CA (NO_x), EMAC, MRI (CO), (Niwa-)SOCOL (CO, NO_x), ULAQ, UMUKCA and WACCM actually incorporate surface emissions. E39CA adopts a different emission scenario for NO_x, assuming continually rising emissions for NO_x until 2015 (for industrialized countries) and 2030 (for developing countries), respectively, followed by stabilization of the emissions.

4.3.4. Stratospheric Aerosol Surface Area Densities and Direct Aerosol-Related Heating

[65] The SPARC aerosol data set is constructed from Stratospheric Aerosol and Gas Experiment (SAGE) profile measurements of aerosols, beginning in 1983. SAGE is a series of three satellites taking remote-sensing profiles of atmospheric composition since 1979. In the SAGE climatology, data before 1983 are constructed based on assumptions of background aerosol and, in the case of Agung, assuming a similar distribution of aerosol as after later volcanic eruptions [*SPARC*, 2006; *Thomason et al.*, 2008]. Four big volcanic events are evident, Agung in 1963, El Chichón in 1982, Nevado del Ruiz in 1985, and Mt. Pinatubo in 1991 (Figure 2). A problem is apparent at high latitudes in the Southern Hemisphere, where the satellite sensor cannot distinguish between sulfate aerosols and PSCs. In these areas, sometimes a very low SAD of sulfate aerosol is assumed. With the exception of (Niwa-)SOCOL (using a combination of SAGE and GISS data), all models use this data set for the REF-B1 simulations. For REF-B2 and REF-B0, background (year-2000) data are used cyclically throughout the simulations.

[66] Aerosols cause a perturbation to the heating/cooling profiles of the troposphere and stratosphere, particularly during volcanic eruption periods, and also cause the Earth's

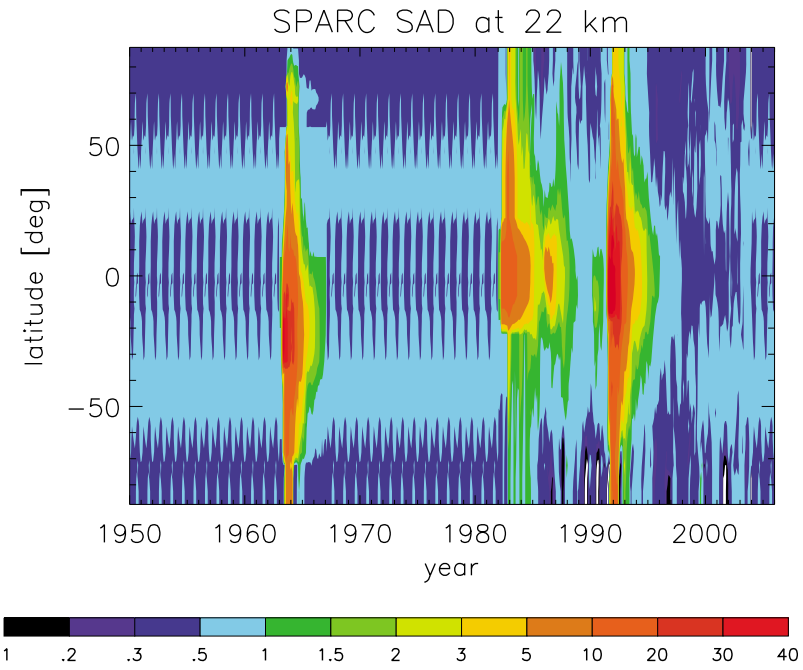

Figure 2. Aerosol surface area density ($\mu m^2/cm^3$) at 22 km, reconstructed from SAGE data. Reproduced from *Morgenstern et al.* [2010b].

surface to warm or cool [*Sato et al.*, 1993]. These effects are associated with a perturbation to the radiative fluxes (such as scattering, reflection into space) associated with the volcanically induced enhancement of the aerosol layer. For example, after the Mt. Pinatubo eruption this led to a global-mean cooling of the Earth' surface [*Robock*, 2002]. Several different approaches have been taken by the CCMVal-2 models regarding this effect: Two models derive heating rates consistent with the prescribed SAD data set (CMAM, WACCM). Others use independent data sets such as the GISS data (AMTRAC3, CCSRNIES, MRI, UMETRAC, UMUKCA-METO). E39CA and EMAC use precalculated rates (G. Stenchikov and L. Oman, as documented by *Eyring et al.* [2008]). The SOCOL models use a mixture of different sources. One (of 4) ULAQ REF-B1 simulations uses estimates of volcanic injections of SO_2, and an interactive aerosol calculation to infer heating rates. The five remaining CCMVal-2 models (CAM3.5, GEOSCCM, LMDZrepro, UMSLIMCAT and UMUKCA-UCAM) do not represent heating due to volcanic aerosol.

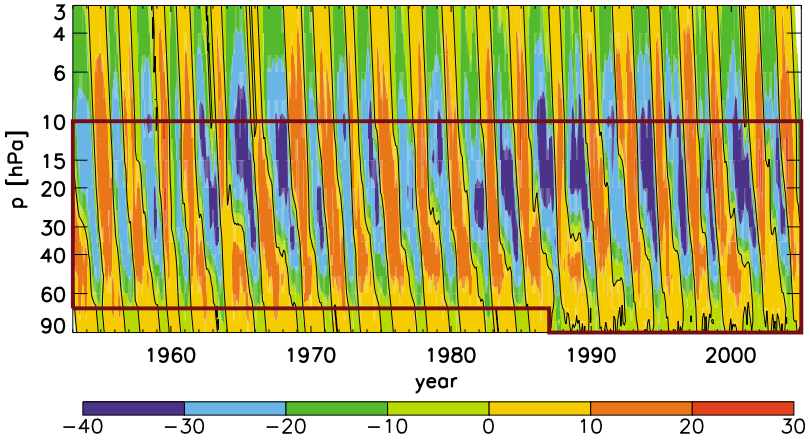

Figure 3. Zonal wind (u) from merged observations at Canton Island, Gan and Singapore, vertically extended (http://www.pa.op.dlr.de/CCMVal/Forcings/qbo_data_ccmval/u_profile_195301-200412.html). The violet box denotes the area constrained by the observations. In the areas outside the box the data are extrapolated, assuming a phase speed of 2 km/month (above 10 hPa) and 1 km/month (below 70 hPa, before 1987). See also *Morgenstern et al.* [2010b].

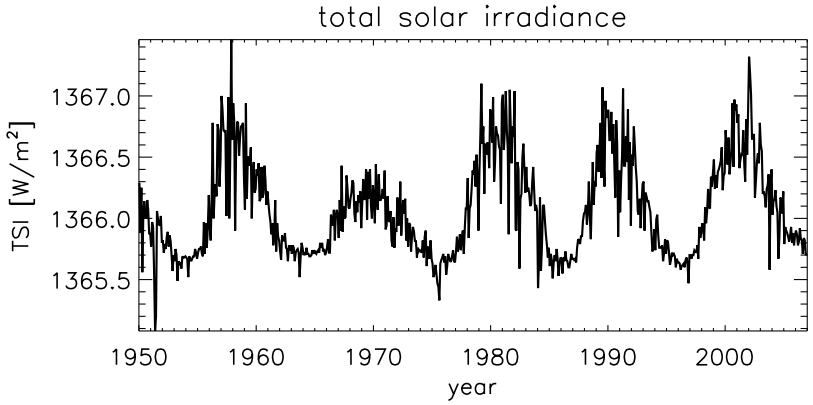

Figure 4. Total solar irradiance (W/m^2) from data of *Lean et al.* [2005] (http://www.geo.fu-berlin.de/en/met/ag/strat/forschung/SOLARIS/Input_data/index.html), updated. Reproduced from *Morgenstern et al.* [2010b].

4.3.5. QBO Time Series

[67] Section 2.1.3 summarizes how the CCMVal-2 models impose the QBO. In those models where the QBO is imposed, generally the data set as displayed in Figure 3 is used as a forcing field.

4.3.6. Solar Irradiance

[68] Solar output varies with sunspot numbers and other parameters. Most of the atmospherically relevant variability is in the 11-year solar cycle. Figure 4 shows total solar irradiance; it varies by about 1 W/m^2 on a background of around 1366 W/m^2. However, most of the variability is at short wavelengths, where the solar cycle is relatively more important than for the spectrally integrated solar output (the "solar constant"). All models except GEOSCCM, ULAQ, UMETRAC, and UMUKCA have implemented the spectrally resolved solar forcing in the REF-B1 simulations, both for radiation and for photolysis calculations. In most cases the solar forcing follows *Lean et al.* [2005].

5. Concluding Remarks

[69] This review of stratospheric CCMs participating in CCMVal-2 has shown that for almost every single process of relevance to stratospheric climate-chemistry modeling, there is a variety of different approaches taken in the CCMs. This diversity complicates the interpretation of any differences found between individual models. Leaving aside the actual performance of models, certain approaches documented here stand out as more physically based or more comprehensive than other approaches. Some models have come closer to the real climate-chemistry system, e.g., regarding the consistent treatment of photolysis and radiation (CAM3.5, CCSRNIES, WACCM). Now three CCMVal-2 models use a comprehensive tropospheric chemistry scheme (CAM3.5, EMAC, ULAQ). This is necessary for addressing questions of how stratospheric ozone changes affect the tropospheric composition [*Stevenson*, 2009; *Hegglin and Shepherd*, 2009], and also for more comprehensively assessing chemical coupling between the two domains. The more widespread adaptation of online photolysis schemes is also in this category. In three models non-orographic gravity-wave deposition account for tropospheric convective activity (CAM3.5, CNRM-ACM, WACCM). For other aspects, some models have become more physically based but the changes involved in this are not thought to make much practical difference in the CCMs considered here, for example the non-hydrostatic dynamical core used by UMUKCA, and the non-family formulation adopted in some CCMVal-2 models.

[70] CMAM is unique among the CCMVal-2 models in that it uses an interactive ocean. The coupling to an ocean must be considered progress because it allows to study the impact of ozone on climate with more confidence than in the other models using prescribed ocean conditions. In those models that do not use an interactive ocean, impacts of ozone changes on lower-tropospheric climate are invariably affected by the lack of feedback from the ocean; this missing feedback complicates the interpretation particularly of lower-tropospheric climate signals. This may be an example of a convergence of CCMVal- and IPCC-type models (CCMs and AOGCMs) such that in the future one category of models (atmosphere-ocean chemistry-climate models) will be used in both climate and ozone assessments. Along similar lines, those models using whole-atmosphere chemistry (CAM3.5, EMAC, ULAQ) may indicate a trend toward comprehensive tropospheric-stratospheric chemistry-climate modeling, such that in the future one category of models will be used to simultaneously cover both stratospheric and tropospheric composition.

[71] **Acknowledgments.** We acknowledge the Chemistry-Climate Model Validation (CCMVal) Activity for WCRP's (World Climate Research Programme) SPARC (Stratospheric Processes and their Role in Climate) project for organizing and coordinating the model data analysis activity, and the British Atmospheric Data Centre (BADC) for collecting and archiving the CCMVal model output. CCSRNIES research was supported by the Global Environmental Research Found of the Ministry of the Environment of Japan (A-071) and the simulations were completed with the supercomputer at CGER, NIES. O.M. acknowledges funding under the DMGC program (contract C01X0703). P.B. has been supported by the UK Natural Environment Research Council (NERC) through the NCAS initiative. UMUKCA-UCAM and UMSLIMCAT simulations made use of the facilities of HECToR, the UK's national high-performance computing service, which is provided by UoE HPCx Ltd. at the University of Edinburgh, Cray Inc. and NAG Ltd., and funded by the Office of Science

and Technology through EPSRC's High End Computing Programme. The National Center for Atmospheric Research is operated by the University Corporation for Atmospheric Research under sponsorship of the National Science Foundation. Any opinions, findings and conclusions or recommendations expressed in the publication are those of the authors and do not necessarily reflect the views of the National Science Foundation. We acknowledge valuable comments by three anonymous reviewers.

References

Adcroft, A., J.-M. Campin, C. Hill, and J. Marshall (2007), Implementation of an atmosphere-ocean general circulation model on the expanded spherical cube, *Mon. Weather Rev.*, *132*, 2845–2863.

Akiyoshi, H., L. B. Zhou, Y. Yamashita, K. Sakamoto, M. Yoshiki, T. Nagashima, M. Takahashi, J. Kurokawa, M. Takigawa, and T. Imamura (2009), A CCM simulation of the breakup of the Antarctic polar vortex in the years 1980–2004 under the CCMVal scenarios, *J. Geophys. Res.*, *114*, D03103, doi:10.1029/2007JD009261.

Alexander, M. J., and T. J. Dunkerton (1999), A spectral parameterization of mean flow forcing due to breaking gravity waves, *J. Atmos. Sci.*, *56*, 4167–4182.

Anstey, J. A., T. G. Shepherd, and J. F. Scinocca (2010), Influence of the quasi-biennial oscillation on the extratropical winter stratosphere in an atmospheric general circulation model and in reanalysis data, *J. Atmos. Sci.*, *67*, 1402–1419.

Arora, V. K., G. J. Boer, J. R. Christian, C. L. Curry, K. L. Denman, K. Zahariev, G. M. Flato, J. F. Scinocca, W. J. Merryfield, and W. G. Lee (2009), The effect of terrestrial photosynthesis down regulation on the twentieth-century carbon budget simulated with the CCCma Earth System model, *J. Clim.*, *22*, 6066–6088.

Austin, J. (1991), On the explicit versus family solution of the fully diurnal photochemical equations of the stratosphere, *J. Geophys. Res.*, *96*, 12,941–12,975.

Austin, J., and N. Butchart (2003), Coupled chemistry-climate model simulations of the period 1980–2020: Ozone depletion and the start of ozone recovery, *Q. J. R. Meteorol. Soc.*, *129*, 3225–3249.

Austin, J., and R. J. Wilson (2006), Ensemble simulations of the decline and recovery of stratospheric ozone, *J. Geophys. Res.*, *111*, D16314, doi:10.1029/2005JD006907.

Austin, J., et al. (2008), Coupled chemistry climate model simulations of the solar cycle in ozone and temperature, *J. Geophys. Res.*, *113*, D11306, doi:10.1029/2007JD009391.

Austin, J., et al. (2010), Chemistry-climate model simulations of spring Antarctic ozone, *J. Geophys. Res.*, doi:10.1029/2009JD013577, in press.

Baldwin, M. P., et al. (2001), The quasi-biennial oscillation, *Rev. Geophys.*, *39*(2), 179–229.

Bian, H., and M. J. Prather (2002), Fast-J2: Accurate simulation of stratospheric photolysis in global chemical models, *J. Atmos. Chem.*, *41*, 281–296.

Bossuet, C., M. Déqué, and D. Cariolle (1998), Impact of a simple parameterization of convective gravity-wave drag in a stratosphere-troposphere general circulation model and its sensitivity to vertical resolution, *Ann. Geophys.*, *16*, 238–249.

Brasseur, G. P., J. J. Orlando, and G. S. Tyndall (1999), *Atmospheric Chemistry and Climate Change*, 688 pp., Oxford Univ. Press, New York.

Buchholz, J. (2005), Simulations of physics and chemistry of polar stratospheric clouds with a general circulation model, Ph.D. thesis, Univ. of Mainz, Mainz, Germany.

Charron, M., and E. Manzini (2002), Gravity waves from fronts: Parameterization and middle atmosphere response in a general circulation model, *J. Atmos. Sci.*, *59*, 923–941.

Chipperfield, M. P. (1999), Multiannual simulations with a three-dimensional chemical transport model, *J. Geophys. Res.*, *104*, 1781–1805.

Collins, W. D., P. J. Rasch, B. A. Boville, J. J. Hack, J. R. McCaa, D. L. Williamson, B. P. Briegleb, C. M. Bitz, S.-J. Lin, and M. Zhang (2006), The formulation and atmospheric simulation of the Community Atmosphere Model: CAM3, *J. Clim.*, *19*, 2122–2161.

Dameris, M., et al. (2005), Long-term changes and variability in a transient simulation with a chemistry-climate model employing realistic forcing, *Atmos. Chem. Phys.*, *5*, 2121–2145.

Davies, T., M. J. P. Cullen, A. J. Malcolm, M. H. Mawson, A. Staniforth, A. A. White, and N. Wood (2005), A new dynamical core for the Met Office's global and regional modelling of the atmosphere, *Q. J. R. Meteorol. Soc.*, *131*, 1759–1782.

de Grandpré, J., J. W. Sandilands, J. C. McConnell, S. R. Beagley, P. C. Croteau, and M. Y. Danilin (1997), Canadian Middle Atmosphere Model: Preliminary results from the chemical transport module, *Atmos. Ocean*, *35*, 385–431.

de Grandpré, J., S. R. Beagley, V. I. Fomichev, E. Griffioen, J. C. McConnell, A. S. Medvedev, and T. G. Shepherd (2000), Ozone climatology using interactive chemistry: Results from the Canadian Middle Atmosphere Model, *J. Geophys. Res.*, *105*, 26,475–26,491.

Delworth, T. L., et al. (2006), GFDL's CM2 global coupled climate models—Part 1: Formulation and simulation characteristics, *J. Clim.*, *19*, 643–674.

DeMore, W. B., S. P. Sander, D. M. Golden, R. F. Hampson, M. J. Kurylo, C. J. Howard, A. R. Ravishankara, C. E. Kolb, and M. J. Molina (1997), Chemical kinetics and photochemical data for use in stratospheric modeling: Evaluation number 12, *JPL Publ.*, *97-4*.

Déqué, M. (2007), Frequency of precipitation and temperature extremes over France in an anthropogenic scenario: Model results and statistical correction according to observed values, *Global Planet. Change*, *57*, 16–26.

Douglass, A. R., R. B. Rood, S. R. Kawa, and D. J. Allen (1997), A three-dimensional simulation of the evolution of middle latitude winter ozone in the middle stratosphere, *J. Geophys. Res.*, *102*, 19,217–19,232.

Dufresne, J.-L., J. Quaas, O. Boucher, F. Denvil, and L. Fairhead (2005), Contrasts in the effects on climate of anthropogenic sulfate aerosols between the 20th and the 21st century, *Geophys. Res. Lett.*, *32*, L21703, doi:10.1029/2005GL023619.

Edwards, J. M., and A. Slingo (1996), Studies with a flexible new radiation code. I: Choosing a configuration for a large scale model, *Q. J. R. Meteorol. Soc.*, *122*, 689–719.

Egorova, T., E. Rozanov, V. Zubov, and I. Karol (2003), Model for investigating ozone trends, *Isv. Russ. Acad. Sci. Atmos. Oceanic Phys., Engl. Transl.*, *39*(3), 277–292.

Eluszkiewicz, J., R. S. Hemler, J. D. Mahlman, L. Bruhwiler, and L. L. Takacs (2000), Sensitivity of age-of-air calculations to the choice of advection scheme, *J. Atmos. Sci.*, *57*, 3185–3201.

Eyring, V., et al. (2006), Assessment of temperature, trace species, and ozone in chemistry-climate model simulations of the recent past, *J. Geophys. Res.*, *111*, D22308, doi:10.1029/2006JD007327.

Eyring, V., et al. (2007), Multimodel projections of stratospheric ozone in the 21st century, *J. Geophys. Res.*, *112*, D16303, doi:10.1029/2006JD008332.

Eyring, V., M. P. Chipperfield, M. A. Giorgetta, D. E. Kinnison, E. Manzini, K. Matthes, P. A. Newman, S. Pawson, T. G. Shepherd, and D. W. Waugh (2008), Overview of the new CCMVal reference and sensitivity simulations in support of upcoming ozone and climate assessments and the planned SPARC CCMVal report, *SPARC Newsl.*, *30*, 20–26.

Fomichev, V. I., J. P. Blanchet, and D. S. Turner (1998), Matrix parameterization of the 15 μm CO_2 band cooling in the middle and upper atmosphere for variable CO_2 concentration, *J. Geophys. Res.*, *103*, 11,505–11,528.

Garcia, R. R., and B. A. Boville (1994), Downward control of the mean meridional circulation and temperature distribution of the polar winter stratosphere, *J. Atmos. Sci.*, *51*, 2238–2245.

Garcia, R. R., D. R. Marsh, D. E. Kinnison, B. A. Boville, and F. Sassi (2007), Simulation of secular trends in the middle atmosphere, 1950–2003, *J. Geophys. Res.*, *112*, D09301, doi:10.1029/2006JD007485.

Gent, P. R., F. O. Bryan, G. Danabasoglu, S. C. Doney, W. R. Holland, W. G. Large, and J. C. McWilliams (1998), The NCAR Climate System Model global ocean component, *J. Clim.*, *11*, 1287–1306.

Gerber, E. P., et al. (2010), Stratosphere-troposphere coupling and annular mode variability in chemistry-climate models, *J. Geophys. Res.*, doi:10.1029/2009JD013770, in press.

Gettelman, A., et al. (2010), Multi-model assessment of the upper troposphere and lower stratosphere: Tropics and global trends, *J. Geophys. Res.*, doi:10.1029/2009JD013638, in press.

Giorgetta, M. A., and L. Bengtsson (1999), Potential role of the quasi-biennial oscillation in the stratosphere-troposphere exchange as found in water vapor in general circulation model experiments, *J. Geophys. Res.*, *104*, 6003–6019.

Giorgetta, M. A., E. Manzini, and E. Roeckner (2002), Forcing of the quasi-biennial oscillation from a broad spectrum of atmospheric waves, *Geophys. Res. Lett.*, *29*(8), 1245, doi:10.1029/2002GL014756.

Giorgetta, M. A., E. Manzini, E. Roeckner, M. Esch, and L. Bengtsson (2006), Climatology and forcing of the quasi-biennial oscillation in the MAECHAM5 model, *J. Clim.*, *19*, 3882–3901.

Gregory, A. R., and V. West (2002), The sensitivity of a model's stratospheric tape recorder to the choice of advection scheme, *Q. J. R. Meteorol. Soc.*, *128*, 1827–1846.

Grewe, V., D. Brunner, M. Dameris, J. Grenfell, R. Hein, D. Shindell, and J. Staehelin (2001), Origin and variability of upper tropospheric nitrogen oxides and ozone at northern mid-latitudes, *Atmos. Environ.*, *35*, 3421–3433.

Hegglin, M. I., and T. G. Shepherd (2009), Large climate-induced changes in ultraviolet index and stratosphere-to-troposphere ozone flux, *Nat. Geosci.*, *2*, 687–691.

Hegglin, M. I., et al. (2010), Multi-model assessment of the upper troposphere and lower stratosphere: Extra-tropics, *J. Geophys. Res.*, doi:10.1029/2010JD013884, in press.

Hines, C. O. (1997a), Doppler-spread parameterization of gravity-wave momentum deposition in the middle atmosphere. Part 1: Basic formulation, *J. Atmos. Sol. Terr. Phys.*, *59*, 371–386.

Hines, C. O. (1997b), Doppler-spread parameterization of gravity-wave momentum deposition in the middle atmosphere. Part 2: Broad and quasi monochromatic spectra, and implementation, *J. Atmos. Sol. Terr. Phys.*, *59*, 387–400.

Hitchcock, P., T. G. Shepherd, and C. McLandress (2009), Past and future conditions for polar stratospheric cloud formation in the Canadian Middle Atmosphere Model, *Atmos. Chem. Phys.*, *9*, 483–495.

Holton, J. R. (1992), *An Introduction to Dynamical Meteorology*, 3rd ed., 511 pp., Academic, San Diego, Calif.

Horinouchi, T., et al. (2003), Tropical cumulus convection and upward-propagating waves in middle-atmospheric GCMs, *J. Atmos. Sci.*, *60*, 2765–2782.

Hough, A. M. (1991), Development of a two-dimensional global tropospheric model: Model chemistry, *J. Geophys. Res.*, *96*, 7325–7362.

Hourdin, F., and A. Armengaud (1999), The use of finite-volume methods for atmospheric advection trace species: 1. Tests of various formulations in a general circulation model, *Mon. Weather Rev.*, *127*, 822–837.

Intergovernmental Panel on Climate Change (IPCC) (2001), *Climate Change 2001: The Scientific Basis: Contribution of Working Group 1 to the Third Assessment Report of the Intergovernmental Panel on Climate Change*, edited by J. T. Houghton et al., 881 pp., Cambridge Univ. Press, New York.

Jacobson, M. Z. (1999), *Fundamentals of Atmospheric Modeling*, 656 pp., Cambridge Univ. Press, Cambridge, U. K.

Jöckel, P., R. von Kuhlmann, M. G. Lawrence, B. Steil, C. A. M. Brenninkmeijer, P. J. Crutzen, P. J. Rasch, and B. Eaton (2001), On a fundamental problem in implementing flux-form advection schemes for tracer transport in 3-dimensional general circulation and chemistry transport models, *Q. J. R. Meteorol. Soc.*, *127*, 1035–1052.

Jöckel, P., et al. (2006), The atmospheric chemistry general circulation model ECHAM5/MESSy1: Consistent simulation of ozone from the surface to the mesosphere, *Atmos. Chem. Phys.*, *6*, 5067–5104. (Available at http://www.atmos-chem-phys.net/6/5067/2006/.)

Johns, T. C., et al. (2006), The new Hadley Centre climate model HadGEM1: Evaluation of coupled simulations, *J. Clim.*, *19*, 1327–1353.

Jourdain, L., S. Bekki, F. Lott, and F. Lefèvre (2008), The coupled chemistry-climate model LMDz-REPROBUS: Description and evaluation of a transient simulation of the period 1980–1999, *Ann. Geophys.*, *26*, 1391–1413.

Kinnison, D. E., et al. (2007), Sensitivity of chemical tracers to meteorological parameters in the MOZART-3 chemical transport model, *J. Geophys. Res.*, *112*, D20302, doi:10.1029/2006JD007879.

Kockarts, G. (1980), Nitric oxide cooling in the terrestrial thermosphere, *Geophys. Res. Lett.*, *7*, 137–140.

Lamarque, J.-F., D. E. Kinnison, P. G. Hess, and F. M. Vitt (2008), Simulated lower stratospheric trends between 1970 and 2005: Identifying the role of climate and composition changes, *J. Geophys. Res.*, *113*, D12301, doi:10.1029/2007JD009277.

Landgraf, J., and P. J. Crutzen (1998), An efficient method for online calculations of photolysis and heating rates, *J. Atmos. Sci.*, *55*, 863–878.

Lanser, D., J. G. Blom, and J. G. Verwer (2000), Spatial discretization of the shallow water equations in spherical geometry using Osher's scheme, *J. Comput. Phys.*, *165*(2), 542–565.

Lary, D. J., and J. A. Pyle (1991), Diffuse radiation, twilight, and photochemistry—I, *J. Atmos. Chem.*, *13*(4), 373–392.

Lean, J., G. Rottman, J. Harder, and G. Kopp (2005), SORCE contributions to new understanding of global change and solar variability, *Sol. Phys.*, *230*, 27–53.

Lefèvre, F., F. Figarol, K. S. Carslaw, and T. Peter (1998), The 1997 Arctic ozone depletion quantified from three-dimensional model simulations, *Geophys. Res. Lett.*, *25*, 2425–2428, doi:10.1029/98GL51812.

Lin, S.-J. (2004), A "vertically Lagrangian" finite volume dynamical core for global models, *Mon. Weather Rev.*, *132*, 2293–2307.

Lin, S.-J., and R. B. Rood (1996), Multi-dimensional flux-form semi-Lagrangian transport schemes, *Mon. Weather Rev.*, *124*, 2046–2070.

Lin, S.-J., and R. B. Rood (1997), An explicit flux-form semi-Lagrangian shallow water model on the sphere, *Q. J. R. Meteorol. Soc.*, *123*, 2531–2533.

Logan, J. A. (1999), An analysis of ozonesonde data for the troposphere: Recommendations for testing 3-D models and development of a gridded climatology for tropospheric ozone, *J. Geophys. Res.*, *104*, 16,115–16,150.

Lott, F., L. Fairhead, F. Hourdin, and P. Levan (2005), The stratospheric version of LMDz: Dynamical climatologies, Arctic Oscillation, and impact on the surface climate, *Clim. Dyn.*, *25*, 851–868, doi:10.1007/s00382-005-0064.

Madec, G., P. Delecluse, M. Imbard, and C. Lévy (1998), OPA version 8.1 ocean general circulation model reference manual, *Notes du Pôle de Modél. 11*, 91 pp., Inst. Pierre-Simon Laplace, Paris.

Marsh, D. R., R. R. Garcia, D. E. Kinnison, B. A. Boville, F. Sassi, S. C. Solomon, and K. Matthes (2007), Modeling the whole atmosphere response to solar cycle changes in radiative and geomagnetic forcing, *J. Geophys. Res.*, *112*, D23306, doi:10.1029/2006JD008306.

McCalpin, J. D. (1988), A quantitative analysis of the dissipation inherent in semi-Lagrangian advection, *Mon. Weather Rev.*, *116*, 2330–2336.

McIntyre, M. E. (1995), The stratospheric polar vortex and sub-vortex: Fluid dynamics and midlatitude ozone loss, *Philos. Trans. R. Soc. London, Ser. A*, *352*, 227–240.

McLandress, C. (2002), Interannual variations of the diurnal tide in the mesosphere induced by a zonal-mean wind oscillation in the tropics, *Geophys. Res. Lett.*, *29*(9), 1305, doi:10.1029/2001GL014551.

McLandress, C., and J. F. Scinocca (2005), The GCM response to current parameterizations of non-orographic gravity wave drag, *J. Atmos. Sci.*, *42*, 2394–2413.

Morgenstern, O., P. Braesicke, F. M. O'Connor, A. C. Bushell, C. E. Johnson, S. M. Osprey, and J. A. Pyle (2009), Evaluation of the new UKCA climate-composition model—Part 1: The stratosphere, *Geosci. Model Dev.*, *2*, 43–57.

Morgenstern, O., et al. (2010a), Anthropogenic forcing of the northern annular mode in CCMVal-2 models, *J. Geophys. Res.*, doi:10.1029/2009JD013347, in press.

Morgenstern, O., et al. (2010b), Chemistry climate models and scenarios, in *SPARC Report on the Evaluation of Chemistry-Climate Models*, edited by V. Eyring, T. G. Shepherd, and D. W. Waugh, *SPARC Rep. 5, WCRP-132, WMO/TD 1526*, pp. 17–70, World Clim. Res. Programme, Geneva, Switzerland.

Mote, P. W., K. H. Rosenlof, M. E. McIntyre, E. S. Carr, J. C. Gille, J. R. Holton, J. S. Kinnersley, H. C. Pumphrey, J. M. Russell III, and J. W. Waters (1996), An atmospheric tape recorder: The imprint of tropical tropopause temperatures on stratospheric water vapor, *J. Geophys. Res.*, *101*, 3989–4006.

Müller, J.-F., and G. Brasseur (1995), IMAGES: A three dimensional chemical transport model of the global troposphere, *J. Geophys. Res.*, *100*, 16,445–16,490.

Nozawa, T., T. Nagashima, T. Ogura, T. Yokohata, N. Okada, and H. Shiogama (2007), *Climate Change Simulations With a Coupled Ocean-Atmosphere GCM Called the Model for Interdisciplinary Research on Climate: MIROC*, *CGER's Supercomput. Monogr. Rep.*, vol. 12, 79 pp., Cent. for Global Environ. Res., Natl. Inst. for Environ. Studies, Tsukuba, Japan.

Numaguti, A., S. Sugata, M. Takahashi, T. Nakajima, and A. Sumi (1997), *Study on the Climate System and Mass Transport by a Climate Model*, *CGER's Supercomput. Monogr. Rep.*, vol. 3, 91 pp., Cent. for Global Environ. Res., Natl. Inst. for Environ. Studies, Tsukuba, Japan.

Olivier, J. G. J., et al. (2005), Recent trends in global greenhouse gas emissions: Regional trends and spatial distribution of key sources, in *Non-CO_2 Greenhouse Gases (NCGG-4)*, edited by A. van Amstel, pp. 325–330, Millpress, Rotterdam, Netherlands.

Pawson, S., R. S. Stolarski, A. R. Douglass, P. A. Newman, J. E. Nielsen, S. M. Frith, and M. L. Gupta (2008), Goddard Earth Observing System chemistry-climate model simulations of stratospheric ozone-temperature coupling between 1950 and 2005, *J. Geophys. Res.*, *113*, D12103, doi:10.1029/2007JD009511.

Pitari, G. (1993), A numerical study of the possible perturbation of stratospheric dynamics due to Pinatubo aerosols: Implications for tracer transport, *J. Atmos. Sci.*, *50*, 2443–2461.

Pitari, G., E. Mancini, V. Rizi, and D. T. Shindell (2002), Impact of future climate and emission changes on stratospheric aerosols and ozone, *J. Atmos. Sci.*, *59*, 414–440.

Price, C., and D. Rind (1992), A simple parameterization for calculating global lightning distributions, *J. Geophys. Res.*, *97*, 9919–9933.

Price, C., and D. Rind (1994), Modeling global lightning distributions in a general-circulation model, *Mon. Weather Rev.*, *122*, 1930–1939.

Priestley, A. (1993), A quasi-conservative version of the semi-Lagrangian advection scheme, *Mon. Weather Rev.*, *121*, 621–629, doi:10.1175/1520-0493.

Putman, W. M., and S.-J. Lin (2007), Finite-volume transport on various cubed-sphere grids, *J. Comput. Phys.*, *227*(1), 55–78.

Ramaroson, R., M. Pirre, and D. Cariolle (1992), A box model for online computations of diurnal variations in a 1-D model—Potential for application in multidimensional cases, *Ann. Geophys.*, *10*, 416–428.

Rasch, P. J., and D. L. Williamson (1990), Computational aspects of moisture transport in global models of the atmosphere, *Q. J. R. Meteorol. Soc.*, *116*, 1071–1090.

Rasch, P. J., D. B. Coleman, N. Mahowald, D. L. Williamson, S.-J. Lin, B. A. Boville, and P. Hess (2006), Characteristics of atmospheric transport using three numerical formulations for atmospheric dynamics in a single GCM framework, *J. Clim.*, *19*, 2243–2266.

Rayner, N. A., D. E. Parker, E. B. Horton, C. K. Folland, L. V. Alexander, D. P. Rowell, E. C. Kent, and A. Kaplan (2003), Global analyses of sea surface temperature, sea ice, and night marine air temperature since the late nineteenth century, *J. Geophys. Res.*, *108*(D14), 4407, doi:10.1029/2002JD002670.

Reithmeier, C., and R. Sausen (2002), ATTILA: Atmospheric tracer transport in a Lagrangian model, *Tellus, Ser. B*, *54*, 278–299.

Richter, J. H., F. Sassi, and R. R. Garcia (2010), Toward a physically based gravity wave source parameterization in a general circulation model, *J. Atmos. Sci.*, *67*, 136–156.

Robock, A. (2002), Pinatubo eruption: The climatic aftermath, *Science*, *295*, 1242–1244.

Roeckner, E., et al. (2003), The atmospheric general circulation model ECHAM5. Part I: Model description, *Rep. 218*, 90 pp., Max-Planck-Inst. für Meteorol., Hamburg, Germany.

Roeckner, E., R. Brokopf, M. Esch, M. Giorgetta, S. Hagemann, L. Kornblueh, E. Manzini, U. Schlese, and U. Schulzweida (2004), The atmospheric general circulation model ECHAM5. Part II: Sensitivity of simulated climate to horizontal and vertical resolution, *Rep. 354*, Max-Planck-Inst. für Meteorol., Hamburg, Germany.

Rozanov, E., M. E. Schlesinger, V. Zubov, F. Yang, and N. G. Andronova (1999), The UIUC three-dimensional stratospheric chemical transport model: Description and evaluation of the simulated source gases and ozone, *J. Geophys. Res.*, *104*, 11,755–11,781.

Sander, S. P., et al. (2002), Chemical kinetics and photochemical data for use in atmospheric studies: Evaluation number 14, *JPL Publ., 02-25*.

Sander, S. P., et al. (2006), Chemical kinetics and photochemical data for use in atmospheric studies: Evaluation number 15, *JPL Publ., 06-2*.

Sato, M., J. E. Hansen, M. P. McCormick, and J. B. Pollack (1993), Stratospheric aerosol optical depths, 1850–1990, *J. Geophys. Res.*, *98*, 22,987–22,994.

Savage, N. H., K. S. Law, J. A. Pyle, A. Richter, H. Nuss, and J. P. Burrows (2004), Using GOME NO_2 satellite data to examine regional differences in TOMCAT model performance, *Atmos. Chem. Phys.*, *4*, 1895–1912.

Scaife, A. A., N. Butchart, C. D. Warner, D. Stainforth, W. Norton, and J. Austin (2000), Realistic quasi-biennial oscillations in a simulation of the global climate, *Geophys. Res. Lett.*, *27*, 3481–3484.

Scaife, A. A., N. Butchart, C. D. Warner, and R. Swinbank (2002), Impact of a spectral gravity wave parametrization on the stratosphere in the Met Office Unified Model, *J. Atmos. Sci.*, *59*, 1473–1489.

Schraner, M., et al. (2008), Technical note: Chemistry-climate model SOCOL—Version 2.0 with improved transport and chemistry/microphysics schemes, *Atmos. Chem. Phys.*, *8*, 5957–5974.

Schultz, M., et al. (2007), Emission data sets and methodologies for estimating emissions, Reanalysis of the tropospheric chemical composition over the past 40 years—A long-term global modeling study of tropospheric chemistry funded under the 5th EU Framework Programme, EU contract EVK2-CT-2002-00170, *Work Package 1*, Eur. Comm., Brussels. (Available at http://retro.enes.org/reports/D1-6_final.pdf.)

Scinocca, J. F. (2003), An accurate spectral nonorographic gravity wave drag parameterization for general circulation models, *J. Atmos. Sci.*, *60*, 667–682.

Scinocca, J. F., N. A. McFarlane, M. Lazare, J. Li, and D. Plummer (2008), Technical note: The CCCma third generation AGCM and its extension into the middle atmosphere, *Atmos. Chem. Phys.*, *8*, 7055–7074.

Shaw, T. A., and T. G. Shepherd (2007), Angular momentum conservation and gravity wave drag parameterization: Implications for climate models, *J. Atmos. Sci.*, *64*, 190–203.

Shepherd, T. G. (2003), Large-scale atmospheric dynamics for atmospheric chemists, *Chem. Rev.*, *103*, 4509–4531.

Shepherd, T. G. (2007), Transport in the middle atmosphere, *J. Meteorol. Soc. Jpn.*, *85B*, 165–191.

Shepherd, T. G. (2008), Dynamics, stratospheric ozone, and climate change, *Atmos. Ocean*, *46*, 117–138, doi:10.3137/ao.460106.

Shepherd, T. G., and T. A. Shaw (2004), The angular momentum constraint on climate sensitivity and downward influence in the middle atmosphere, *J. Atmos. Sci.*, *61*, 2899–2908.

Shepherd, T. G., K. Semeniuk, and J. N. Koshyk (1996), Sponge layer feedbacks in middle-atmosphere models, *J. Geophys. Res.*, *101*, 23,447–23,464.

Shibata, K., and M. Deushi (2008a), Long-term variations and trends in the simulation of the middle atmosphere 1980–2004 by the chemistry-climate model of the Meteorological Research Institute, *Ann. Geophys.*, *26*, 1299–1326.

Shibata, K., and M. Deushi (2008b), *Simulation of the Stratospheric Circulation and Ozone During the Recent Past (1980–2004) With the MRI Chemistry-Climate Model*, *CGER's Supercomput. Monogr. Rep.*, vol. 13, 154 pp., Cent. for Global Environ. Res., Natl. Inst. for Environ. Studies, Tsukuba, Japan.

Shiogama, H., M. Watanabe, M. Kimoto, and T. Nozawa (2005), Anthropogenic and natural forcing impacts on ENSO-like decadal variability during the second half of the 20th century, *Geophys. Res. Lett.*, *32*, L21714, doi:10.1029/2005GL023871.

Son, S.-W., L. M. Polvani, D. W. Waugh, H. Akiyoshi, R. Garcia, D. Kinnison, S. Pawson, E. Rozanov, T. G. Shepherd, and K. Shibata (2008), The impact of stratospheric ozone recovery on the Southern Hemisphere westerly jet, *Science*, *320*, 1486–1489, doi:10.1126/science.1155939.

Steil, B., M. Dameris, C. Brühl, P. J. Crutzen, V. Grewe, M. Ponater, and R. Sausen (1998), Development of a chemistry module for GCMs: First results of a multiannual integration, *Ann. Geophys.*, *16*, 205–228.

Stenke, A., V. Grewe, and M. Ponater (2008), Lagrangian transport of water vapor and cloud water in the ECHAM4 GCM and its impact on the cold bias, *Clim. Dyn.*, *31*, 491–506.

Stenke, A., M. Dameris, V. Grewe, and H. Garny (2009), Implications of Lagrangian transport for coupled chemistry-climate simulations, *Atmos. Chem. Phys.*, *9*, 5489–5504.

Stevenson, D. S. (2009), Atmospheric science: Putting the wind up ozone, *Nat. Geosci.*, *2*, 677–679.

Stott, P., G. Jones, J. Lowe, P. Thorne, C. Durman, T. Johns, and J. Thelen (2006), Transient climate simulations with the HadGEM1 climate model: Causes of past warming and future climate change, *J. Clim.*, *19*, 2763–2782.

Stratospheric Processes and Their Role in Climate (SPARC) (2006), Assessment of Stratospheric Aerosol Properties (ASAP), *Tech. Rep. WMO-TD 1295, WCRP Ser. Rep. 124, SPARC Rep. 4*, World Clim. Res. Programme, Geneva, Switzerland.

Struthers, H., G. E. Bodeker, D. Smale, E. Rozanov, M. Schraner, and T. Peter (2009), Evaluating how photochemistry and transport determine stratospheric inorganic chlorine in coupled chemistry-climate models, *Geophys. Res. Lett.*, *36*, L04805, doi:10.1029/2008GL036403.

Takahashi, M. (1999), Simulation of the quasi-biennial oscillation in a general circulation model, *Geophys. Res. Lett.*, *26*, 1307–1310.

Taylor, K. E., D. Williamson, and F. Zwiers (2000), The sea surface temperature and sea-ice concentration boundary conditions for AMIP II simulations, *Rep. 60*, Program for Clim. Model Diagnosis and Intercomparison, Livermore, Calif.

Teyssèdre, H., et al. (2007), A new tropospheric and stratospheric chemistry and transport model MOCAGE-Climat for multi-year studies: Evaluation of the present-day climatology and sensitivity to surface processes, *Atmos. Chem. Phys.*, *7*, 5815–5860.

Tian, W., and M. P. Chipperfield (2005), A new coupled chemistry-climate model for the stratosphere: The importance of coupling for future O_3-climate predictions, *Q. J. R. Meteorol. Soc.*, *131*, 281–303.

Thomason, L. W., S. P. Burton, B.-P. Luo, and T. Peter (2008), SAGE II measurements of stratospheric aerosol properties at non-volcanic levels, *Atmos. Chem. Phys.*, *8*, 983–995.

van Aardenne, J. A., F. J. Dentener, J. G. J. Olivier, C. G. M. Klein Goldewijk, and J. Lelieveld (2001), A 1° × 1° resolution data set of historical anthropogenic trace gas emissions for the period 1890–1990, *Global Biogeochem. Cycles*, *15*(4), 909–928.

Vogel, B., P. Konopka, J.-U. Grooss, R. Müller, B. Funke, M. Lopez-Puertas, T. Reddmann, G. Stiller, T. von Clarmann, and M. Riese (2008), Model simulations of stratospheric ozone loss caused by enhanced mesospheric NO_x during Arctic winter 2003/2004, *Atmos. Chem. Phys.*, *8*, 5279–5293.

Walcek, C. J., R. A. Brost, J. S. Chang, and M. L. Wesely (1986), SO_2, sulfate and HNO_3 deposition velocities computed using regional landuse and meteorological data, *Atmos. Environ.*, *20*, 949–964.

Warner, C. D., and M. E. McIntyre (2001), An ultrasimple spectral parameterization for non-orographic gravity waves, *J. Atmos. Sci.*, *58*, 1837–1857.

Williamson, D. L., and P. J. Rasch (1989), Two-dimensional semi-Lagrangian transport with shape-preserving interpolation, *Mon. Weather Rev.*, *117*, 102–129.

World Meteorological Organization (WMO) (2007), *Scientific Assessment of Ozone Depletion: 2006*, *Global Ozone Res. Monit. Proj. Rep. 50*, 572 pp., Geneva, Switzerland.

Xiao, F., and X. Peng (2004), A convexity preserving scheme for conservative advection transport, *J. Comput. Phys.*, *198*(2), 389–402, doi:10.1016/j.jcp.2004.01.013.

Yukimoto, S., A. Noda, A. Kitoh, M. Hosaka, H. Yoshimura, T. Uchiyama, K. Shibata, O. Arakawa, and S. Kusunoki (2006), Present-day climate

and climate sensitivity in the Meteorological Research Institute coupled GCM version 2.3 (MRI-CGCM2.3), *J. Meteorol. Soc. Jpn.*, *84*, 333–363.
Zubov, V., E. Rozanov, and M. Schlesinger (1999), Hybrid scheme for three-dimensional advective transport, *Mon. Weather Rev.*, *127*, 1335–1346.

H. Akiyoshi, T. Nakamura, and Y. Yamashita, National Institute of Environmental Studies, Tsukuba, Ibaraki 305-8506, Japan.

J. Austin, National Oceanic and Atmospheric Administration, Princeton, NJ 08540, USA.

A. J. G. Baumgaertner and C. Brühl, Max-Planck-Institut für Chemie, D-55020 Mainz, Germany.

S. Bekki, D. Cugnet, and M. Marchand, LATMOS, IPSL, UVSQ, UPMC, CNRS, INSU, F-75231 Paris, France.

P. Braesicke, NCAS-Climate-Chemistry, Centre for Atmospheric Science, Department of Chemistry, Cambridge University, Cambridge CB2 IEW, UK.

M. P. Chipperfield, S. Dhomse, and W. Tian, School of Earth and Environment, University of Leeds, Leeds LS2 9JT, UK.

M. Dameris, V. Eyring, H. Garny, and P. Jöckel, Deutsches Zentrum für Luft- und Raumfahrt, Institut für Physik der Atmosphäre, D-82234 Wessling, Germany.

S. M. Frith and J. E. Nielsen, NASA Goddard Space Flight Center, Greenbelt, MD 20771, USA.

A. Gettelman, D. E. Kinnison, and J.-F. Lamarque, National Center for Atmospheric Research, Boulder, CO 80305, USA.

M. A. Giorgetta, Max-Planck-Institut für Meteorologie, D-20146 Hamburg, Germany.

S. C. Hardiman, Hadley Centre, Met Office, Exeter EX1 3PB, UK.

M. I. Hegglin and T. G. Shepherd, Department of Physics, University of Toronto, Toronto, ON M5S 1A7, Canada.

E. Mancini and G. Pitari, Dipartimento di Fisica, Università degli Studi dell'Aquila, I-67100 L'Aquila, Italy.

E. Manzini, Centro Euro-Mediterraneo per i Cambiamenti Climatici, I-40127 Bologna, Italy.

M. Michou, D. Olivié, and H. Teyssèdre, GAME, CNRM, Météo-France, CNRS, F-31057 Toulouse, France.

O. Morgenstern and D. Smale, National Institute of Water and Atmospheric Research, Lauder, Private Bag 50061, Omakau, 9352, New Zealand. (o.morgenstern@niwa.co.nz)

D. A. Plummer and J. F. Scinocca, Canadian Centre for Climate Modeling and Analysis, Environment Canada, Victoria, BC V8W 3V6, Canada.

E. Rozanov, Physical-Meteorological Observatory/World Radiation Center, CH-7260 Davos, Switzerland.

K. Shibata, Meteorological Research Institute, Japan Meteorological Agency, Tsukuba, Ibaraki 305-0052, Japan.

M. Toohey, Leibniz-Institut für Meereswissenschaften an der Universität Kiel (IFM-GEOMAR), D-24148 Kiel, Germany.

D. W. Waugh, Department of Earth and Planetary Sciences, John Hopkins University, Baltimore, MD 21218, USA.